III. ATOMS AND RADIATION

1. Definitions; Einstein Coefficients

Consider a transition between states n' and n'': the spontaneous transition probability is $\mathrm{A}_{n'n''}$ s^{-1} for a downward transition $n' \rightarrow n''$ at frequency $\nu = (E_{n'} - E_{n''})/h$. (Conventionally, the upper state of a transition is denoted with a single prime, and the lower state with a double prime.) The mean lifetime against spontaneous decay of the upper state n' is given by:

$$\tau_{n'}^{-1} = \sum_{n''} A_{n'n''} \quad [\mathrm{s}^{-1}] \tag{3.1}$$

where the summation extends over all possible downward transitions from n'. Einstein (1917, *Phys. Zeits.* **18**, 121) defined two other factors that describe the interaction of the radiation field and the transition. The radiation field is said to have an intensity $I_\nu d\nu$ [erg cm^{-2} s^{-1} sr^{-1}] in the frequency interval $d\nu$ about ν. The absorption coefficient $B_{n''n'}$ gives the rate at which upward transitions occur $n'' \rightarrow n'$ in this radiation field at ν:

$$\mathrm{N}(n'')B_{n''n'}I_\nu \quad [\mathrm{s}^{-1}] \tag{3.2}$$

where $\mathrm{N}(n'')$ is the number of atoms initially in state n''. The radiation field also produces induced downward transitions $n' \rightarrow n''$ (called "stimulated emission") at the same frequency at a rate:

$$\mathrm{N}(n')B_{n'n''}I_\nu \quad [\mathrm{s}^{-1}] \tag{3.3}$$

The Einstein coefficients $A_{n'n''}$, $B_{n'n''}$ and $B_{n''n'}$ are inherent properties of an atom independent of the radiation field. Thus we can arbitrarily choose a specific radiation field for the purpose of determining the relationships between these coefficients. It is most useful to consider the case of thermodynamic equilibrium (TE), in which the intensity of radiation is given by the Planck function:

$$I_\nu = B_\nu(\mathrm{T}) = \frac{2hv^3}{c^2} \cdot \frac{1}{e^{-h\nu/k\mathrm{T}} - 1} \tag{3.4}$$

and the same temperature characterizes the relative populations of all energy states. Then we can apply the principle of "detailed balance" (also called "microscopic reversibility"), which states that in TE, the rate of upward transitions must exactly match the rate of the corresponding downward transition. (Otherwise, the system is not is equilibrium!) In TE, the relative state populations are given by the Boltzmann formula:

$$\mathrm{N}(n')/\mathrm{N}(n'') = \frac{g_{n'}}{g_{n''}} e^{-[(E_{n'} - E_{n''})/kT]} \quad , \tag{3.5}$$

where g_n is the statistical weight factor (degeneracy) of state n. Thus, detailed balance requires:

$$\mathrm{N}(n'')B_{n''n'}I_\nu = \mathrm{N}(n')[A_{n'n''} + B_{n'n''}I_\nu] \ . \tag{3.6}$$

From these considerations, it is possible to derive explicit relations between $B_{n'n''}$ and $B_{n''n'}$, and between $A_{n'n''}$ and $B_{n''n'}$, that are independent of T (i.e., that are intrinsic properties of the atom only). We find Einstein's relations:

$$\begin{aligned} g_{n'} B_{n''n'} &= g_{n''} B_{n'n''} \\ A_{n'n''} &= \frac{2h\nu^3}{c^2} B_{n'n''} \quad . \end{aligned} \tag{3.7}$$

The absorption coefficient $B_{n''n'}$, as defined above, must have units [erg^{-1} cm^2 Hz sr] in order for $I_\nu B_{n''n'}$ to have units of an absorption rate in s^{-1}. $B_{n''n'}$ refers to the total rate of an absorption $n'' \rightarrow n'$ of central frequency $\nu_{n''n'}$; it can therefore also be related to the integral over frequency of an absorption cross section, where

$$\sigma_{abs} = \frac{\text{energy absorbed (unit frequency)}^{-1}}{\text{incident flux (unit frequency)}^{-1}} \qquad [\text{cm}^2]. \tag{3.8}$$

Then:

$$\frac{h\nu}{4\pi} B_{n''n'} = \int_0^\infty \sigma_{abs} d\nu \qquad [\text{cm}^2\text{Hz}] \quad . \tag{3.9}$$

The absorption oscillator strength $f_{n''n'}$ was defined originally as:

$$f_{n''n'} = \frac{\int_0^\infty \sigma_{abs}^{QM} \, d\nu}{\int_0^\infty \sigma_{abs}^{CL} \, d\nu} \tag{3.10}$$

i.e., $f_{n''n'}$ is the number of equivalent classical electron oscillators of the same frequency as the transition that would be required to produce the same total absorption. It can be shown that:

$$\int_0^\infty \sigma_{abs} \, d\nu = \frac{\pi e^2}{m_e c} f_{n''n'} \tag{3.11}$$

so that

$$\frac{h\nu}{4\pi} B_{n''n'} = \frac{\pi e^2}{m_e c} f_{n''n'}$$

or

$$\begin{aligned} A_{n'n''} &= \frac{8\pi^2 e^2}{m_e c} \left(\frac{\nu}{c}\right)^2 f_{n''n'} \\ &= 0.66702 \left(\frac{\nu}{c}\right)^2 g_{n''} f_{n''n'} / g_{n'} \quad . \end{aligned} \tag{3.12}$$

For a more complete derivation, see J. D. Jackson, Chapter 17.

2. Multipole expansion of the radiation field

In the semi-classical theory of radiation, the atom is treated quantum mechanically, but the radiation field classically. The Hamiltonian therefore consists of several parts:

$$\mathcal{H} = H_{radiation} + H_{atom} + H_{interaction} \tag{3.13}$$

and its relativistically invariant form may be written as

$$\mathcal{H}(\vec{r},t) \;=\; \frac{1}{2m_e}\left(\vec{p}-\frac{e}{c}\vec{A}\right)^2 \;+\; [V(\vec{r})+e\phi] \quad .$$

$\vec{A}$ is the vector potential and ϕ the scalar potential associated with the electromagnetic field (For those interested in a full treatment of the light-matter interaction, a thorough treatment of E&M may be found in *Classical Electrodynamics* by J.D. Jackson. The book entitled *Quantum Theory* by D. Bohm is a good place to look for detailed discussions of points that are simply asserted here.). Expanding the squared terms yields a time-dependent Schrödinger equation of the form (using $\vec{p}=(\hbar/\imath)\vec{\nabla}$)

$$\mathcal{H}|\Psi> \;=\; \left\{\frac{1}{2m_e}\left(-\hbar^2\vec{\nabla}^2+\imath\hbar\frac{e}{c}\vec{\nabla}\cdot\vec{A}+\imath\hbar\frac{e}{c}\vec{A}\cdot\vec{\nabla}+\frac{e^2}{c^2}|\vec{A}|^2\right)+V(\vec{r})+e\phi\right\}|\Psi>$$

$$=-\frac{\hbar}{\imath}\frac{\partial}{\partial t}|\Psi> \quad .$$

The time dependence of the radiation field arises in the vector potential, which can be written (in complex and real representations)

$$\vec{A}(\vec{r},\omega) \;=\; \vec{A}(\omega)e^{\imath\vec{k}\cdot\vec{r}} \;=\; \vec{A}_0 cos(\omega t-\vec{k}\cdot\vec{r}) \quad ,$$

which leads to electric and magnetic fields given by (real terms)

$$\mathcal{E}(\vec{r},t) \;=\; -\frac{1}{c}\frac{\partial\vec{A}}{\partial t} \;=\; k\vec{A}_0 sin(\omega t-\vec{k}\cdot\vec{r})$$

$$\mathcal{B}(\vec{r},t) \;=\; \vec{\nabla}\times\vec{A} \;=\; \vec{k}\times\vec{A}_0 sin(\omega t-\vec{k}\cdot\vec{r})$$

(remember that $\mathcal{B}$ is in phase with the electric field, but is oriented perpendicularly to $\mathcal{E}$ in a spatial sense).

It turns out that we are free to pick a reference frame, or gauge, in which the problem is as simple as possible. For light-matter interactions, this is called the *Coulomb gauge*, in which the scalar potential is zero and in which the divergence of the vector potential is also zero, that is, $\phi=0$ and $\vec{\nabla}\cdot\vec{A}=0$. In this gauge, the relativistically invariant Schrödinger equation reduces to

$$\mathcal{H}|\Psi> \;=\; \left\{\left[-\frac{\hbar^2}{2m_e}\vec{\nabla}^2+V(\vec{r})\right]+\left[\frac{\imath e\hbar}{2m_e c}\vec{A}\cdot\vec{\nabla}+\frac{e^2}{2m_e c^2}|\vec{A}|^2\right]\right\}|\Psi> \qquad (3.14)$$

In most instances the $|\vec{A}|^2$ term can be neglected, unless very high electromagnetic field intensities are involved (such as can be the case with lasers, particularly ultrafast laser pulses of picosecond or femtosecond duration), and we are left with

$$H_{interaction} \;=\; \frac{\imath e\hbar}{2m_e c}\vec{A}\cdot\sum\vec{\nabla}_j \quad . \qquad (3.15)$$

The probability for a transition per unit time is given by:

$$W_{a\to b} \;=\; \frac{4\pi^2 e^2}{m_e^2 c^2}|A(\omega_{ba})|^2| < b|e^{\imath\vec{k}\cdot\vec{r}}\cdot\sum\vec{\nabla}_j|a>|^2 \tag{3.16}$$

with

$$D_{\rm ba} \;\equiv\; < b|e^{\imath\vec{k}\cdot\vec{r}}\cdot\sum\vec{\nabla}_j|a> \quad . \tag{3.17}$$

The "multipole expansion" consists of expanding $e^{\imath\vec{k}\cdot\vec{r}}$ in a power series:

$$e^{\imath\vec{k}\cdot\vec{r}} \;=\; 1 \;+\; \imath\vec{k}\cdot\vec{r} \;-\; (\vec{k}\cdot\vec{r})^2 \;-\; \imath(\vec{k}\cdot\vec{r})^3/6 \;+\; ... \tag{3.18}$$

The matrix elements D_{ba} are best evaluated one at a time. Assume also for a moment that $j = 1$. If the radiation field is assumed to be z polarized, then, for example, the x-component becomes:

$$(D_{ba})_x \;=\; < b|e^{ikz}\frac{\partial}{\partial x}|a> \quad . \tag{3.19}$$

The electric dipole approximation consists of retaining only the first term in (3.18), $e^{\imath\vec{k}\cdot\vec{r}} \approx 1$. (3.19) then becomes:

$$(D_{ba})_x \;=\; < b|\frac{\partial}{\partial x}|a> \quad . \tag{3.20}$$

This matrix element can be rewritten in terms of the dipole moment operator by using the relation:

$$< b|\frac{\partial}{\partial x}|a> \;=\; -\frac{m_e}{\hbar}(E_b - E_a) < b|x|a> \quad . \tag{3.21}$$

Generalizing this result to the other components, and using $\omega_{ba} = (E_b - E_a)/\hbar$, we find:

$$W_{a\to b} \;=\; \frac{\omega^2}{c^2h^2}|A(\omega_{ba})|^2| < b|x|a>|^2 \;=\; \frac{\omega^2}{c^2h^2e^2}|A(\omega_{ba})|^2| < \vec{d}>| \quad , \tag{3.22}$$

since the electric dipole operator is defined as:

$$\vec{d} \;\equiv\; e\sum\vec{r}_j \quad . \tag{3.23}$$

In cases where the matrix elements of the electric dipole operator vanish, successively higher terms of the expansion (3.18) need to be retained. For example, if the term ikz is included, we find:

$$(D_{ba})_x \;\propto\; < b|z\frac{\partial}{\partial x}|a> \quad . \tag{3.24}$$

To evaluate this term, we divide it in two parts, and add and subtract terms involving $x\frac{\partial}{\partial z}$. Thus,

$$(D_{ba})_x \;\propto\; \left[< b|z\frac{\partial}{\partial x} \;+\; x\frac{\partial}{\partial z}|a> \;+\; < b|z\frac{\partial}{\partial x} \;-\; x\frac{\partial}{\partial z}|a>\right]/2 \quad . \tag{3.25}$$

Using relation (3.21), the first term can be shown to be the xz-component of the quadrupole moment tensor of the molecule:

$$< b|z\frac{\partial}{\partial x} \; + \; x\frac{\partial}{\partial z}|a > \; = \; -\frac{m_e}{\hbar}\omega_{ba} < b|xz|a > \quad . \tag{3.26}$$

The second term in (3.25) has the form of an angular momentum operator, so that:

$$< b|z\frac{\partial}{\partial x} \; - \; x\frac{\partial}{\partial z}|a > \; \propto \; \imath < b|\mu_y|a > \; , \tag{3.27}$$

where μ_y is the y-component of the magnetic dipole moment. Thus, the second-order terms give rise to (part of the) electric quadrupole and (all of the) magnetic dipole radiation. Since they arise from the same expansion term, they are fundamentally of the same order of magnitude.

In summary, in the multipole expansion of $e^{\imath\vec{k}\cdot\vec{r}}$, the first term, the electric dipole term, gives matrix elements of the form:

$$E_1 : \quad < b|\sum_j \vec{r}_j|a > \quad . \tag{3.28}$$

The next term gives both magnetic dipole transition matrix elements

$$M_1 : \quad < b|\sum_j \vec{\mu}_j|a > \tag{3.29}$$

$$E_2 : \quad < b|\sum_j \vec{Q}_j|a > \; , \tag{3.30}$$

where the "electric quadrupole" moment operator is:

$$\vec{Q} \; = \; \vec{r}\cdot\vec{r} \; - \; r^2\delta_{ij}/3 \; . \tag{3.31}$$

Even higher order transitions are sometimes observed: for example, electric hexadecapole transitions in solid hydrogen have been seen in the laboratory and one day might be discovered in some astrophysical region.

3. Selection rules

Consider transitions from state a to state b
$|a> = |\alpha_a J_a M_a>$; $|b> = |\alpha_b J_b M_b>$
where α stands for n, L, M_L, ... For the different terms in the multipole expansion, transition matrix elements vanish identically unless certain "selection rules" are satisfied.

Electric dipole (E_1): The following rules are rigorous in all cases:

$\Delta J = 0, \pm 1$, but $J_a \; = \; 0 \rightarrow J_b$=0 forbidden	
$\Delta M = 0, \pm 1$	(for Stark and Zeeman splittings)
parity must change	$(\Delta \sum l_i = \pm 1)$

The following additional rules hold in **pure** LS coupling
with no configuration interaction:

$\Delta M_L = 0, \pm 1$ (for sublevels)
single electron transitions only (Δl=± 1)
$\Delta L = 0, \pm 1$, but $L_a = 0 \rightarrow L_b = 0$ forbidden
$\Delta S = 0$

These rules are relaxed for deviations from *pure* LS coupling,
or when states contain admixtures of more than one configuration.

Magnetic Dipole (M_1):

$\Delta J = 0, \pm 1$, but $J_a = 0 \rightarrow J_b$=0 forbidden
$\Delta M = 0, \pm 1$ (only important for external fields)
no parity change

The above rules are *rigorous*. In strict LS coupling
there are no M_1 transitions such that:

$\Delta n = 0$
$\Delta l = 0$
$\Delta S = 0$
$\Delta L = 0$

That is, only if the spin-orbit interaction is included can M_1
transitions occur between levels of the same term.

Electric Quadrupole (E_2):

ΔJ =0, ± 1, ± 2
(with $J_a + J_b \geq 2$)
$\Delta M = 0, \pm 1, \pm 2$ (for Stark and Zeeman experiments)
no parity change.

Again, these rules are rigorous. In strict LS coupling they become:

$\Delta S = 0$
$\Delta L = 0, \pm 1, \pm 2$
(with $L_a + L_b \geq 2$)
$\Delta l = 0, \pm 2$, but $l_{\rm a} \rightarrow l_{\rm b} = 0$ forbidden.

Angular distributions:

The transitions with ΔM =0, ± 1, ± 2 for E_1, M_1 or E_2 occur
with equal probability and the net result is independent of angle.

4. Transition probabilities

Consider a transition from a to b, where a is the upper state and b the lower state. Let $|a> = |\alpha_a J_a M_a>$, etc.

(a) Electric dipole transitions

The spontaneous transition probability is

$$(2J_a \ + \ 1)A_{ab} \quad = \quad \frac{64\pi^4\nu^3}{3hc^3}\left[\sum_{M_a}\sum_{M_b}| < \alpha_b J_b M_b|\vec{\alpha}|\alpha_a J_a M_a > |^2\right] \tag{3.32}$$

and S_{ab} is called the "line strength" which is defined as:

$$S_{ab} \quad = \quad \sum_{M_a}\sum_{M_b}| < \alpha_b J_b M_b|\vec{\alpha}|\alpha_a J_a M_a > |^2 \tag{3.33}$$

When S is in atomic units (i.e. $e^2a_0^2$=6.4606 $\times$ 10^{-36} [esu cm]^2):

$$A_{ab} \quad = \quad 2.0261 \times 10^{-6}\tilde{\nu}^3\frac{S_{ab}}{(2J_a \ + \ 1)} \qquad [\mathrm{s}^{-1}] \ , \tag{3.34}$$

where ν is the frequency of the transition in Hz, ν=$|E_a - E_b|/h$=$c\tilde{\nu}$, and $\tilde{\nu}$ is the wavenumber in cm^{-1}. As we have seen before, the absorption oscillator strength f_{ba} and A_{ba} are related by:

$$\begin{aligned}(2J_a \ + \ 1)A_{ab} \quad &= \quad \frac{8\pi^2e^2\nu^2}{m_ec^3}(2J_b \ + \ 1)f_{ab} \\ &= \quad 0.66702\tilde{\nu}^2(2J_b \ + \ 1)f_{ba} \ ,\end{aligned} \tag{3.35}$$

where f_{ba} is dimensionless. Note the notation f_{ba}, where the lower state is listed first. This is the convention for **atoms**; as we will see, for molecules, the order is reversed.

Another useful property is the radiative lifetime of state a:

$$\tau_a \quad = \quad \sum_b A_{ab}^{-1} \qquad [\mathrm{s}] \tag{3.36}$$

where the summation extends over all possible transitions to lower states b. The significance of a lifetime of an excited state is obvious, but there is an additional related physical property that arises from applications of the uncertainty principle:

$$\Delta E_a\tau_a \ \sim \ h \tag{3.37}$$

which implies that the energy of a state a is determined only within an interval $\Delta E_a \ \sim \ h/\tau_a$ about E_a, the nominal eigenvalue. Alternatively, this means that any transition will have a minimum spread in frequency $\Delta\nu \sim 1/\tau_a$ [Hz] about the nominal line center frequency.

Orders of magnitude:

For a strong transition, $S_{ab} = 1$ au. In the visible region, $\nu \simeq 20{,}000\text{cm}^{-1}$

$A \simeq 1.6 \times 10^7$ s^{-1}
$\tau \simeq 62 \times 10^{-9}$ s (62 ns)
$\Delta\nu/\nu \simeq 2.7 \times 10^{-8}$
$f \simeq 0.06$ if $J_a = J_b$

(b) Magnetic dipole transitions

In LS coupling, M_1 transitions can take place only between two levels of the same term. The formula is similar to that for E_1 transitions:

$$A(\alpha_a J_a,\ \alpha_b J_b) \quad = \quad \frac{64\pi^4\nu^3}{3hc^3} \cdot \frac{S_m(\alpha_a J_a,\ \alpha_b, J_b)}{(2J_a\ +\ 1)} \qquad [\text{s}^{-1}] \tag{3.38}$$

where

$$S_m(\alpha_a J_a,\ \alpha_b J_b) \quad = \quad S_m(\alpha_b J_b,\ \alpha_a J_a) \quad = \quad \sum_{M_a}\sum_{M_b} | < \alpha_a J_b M_b | \vec{\mu} | \alpha_a J_a M_a > |^2 \tag{3.39}$$

$$\vec{\mu} \quad = \quad -\frac{e\hbar}{2m_e c}(\vec{L}\ +\ g_e\vec{S}) \tag{3.40}$$

In LS coupling, the line strength for a $L_a = L_b$, $S_a = S_b$, $n_a = n_b$ and $J + 1 \leftrightarrow J$ line is:

$$S_m(SLJ,\ SLJ+1) = \frac{(J-S+L+1)(J+S-L+1)(J+S+L+2)(S+L-J)}{4(J+1)} \tag{3.41}$$

in units of $(e\hbar/2m_e c)^2$.

Recall that the hyperfine transition at λ 21 cm in the ground state of H is a magnetic dipole transition in which $\Delta J = 0$. The spontaneous transition probability for a transition $F \to F - 1$ can be written:

$$A(F, F-1) = \frac{64\pi^4\nu^3}{8\hbar c^3} \cdot \frac{g^2\mu_0^2(g_e/2)^2}{(2F+1)} \cdot$$

$$\frac{(F+J-I)(F+I-J)(I+J+F+1)(I+F-J+1)}{4F} \qquad [\text{s}^{-1}] \tag{3.42}$$

where g is the Landé g factor (not to be confused with the g_e or g_N factors!), or

$$g = [1 + \frac{S(S+1)\ -\ L(L+1)\ +\ J(J+1)}{2J(J+1)} \tag{3.43}$$

(c) Electric quadrupole transitions

$$A_Q(\alpha_a J_a,\ \alpha_b J_b) \quad = \quad \frac{32\pi^6\nu^5}{5hc^5} \cdot \frac{S_Q(\alpha_a J_a,\ \alpha_b J_b)}{(2J_a+1)} \tag{3.44}$$

where

$$S_Q \quad = \quad \sum_{M_b} \sum_{M_a} | < \alpha_b J_b M_b | Q | \alpha_a J_a M_a > |^2 \tag{3.45}$$

and Q is the quadrupole moment operator.

References see C. Mendoza 1983 in "Planetary Nebulae", *IAU Symposium* No. 103 (Reidel, Dordrecht), p.143 for an excellent current review of transition probabilities for most forbidden (M_1 and E_2) transitions of astrophysical interest, as well as for some important E_1 transitions.

(d) Sum rules

There are some general sum rules for oscillator strengths, the most well-known of which is:

$$\sum_n f_{mn} \quad = \quad N \quad = \quad \text{number of electrons in the atom} \tag{3.46}$$

and the sum extends over a complete set of eigenstates; therefore it implicitly includes integration over the *continuum*. Another sum rule is:

$$\sum_n (f_{mn}/E_{mn}^2) \quad = \quad \alpha_m \tag{3.47}$$

where α_m is the polarizability of the system in level m in a.u. and E_{mn} is in a.u.

(e) Determination of transition probabilities

The determination of oscillator strengths and transition probabilities is a vast and complicated subject. It is essential to have accurate values in order to determine abundances and use lines as diagnostics of physical conditions in astronomical objects.

(i) Theoretical methods

The accuracy and applicability of a particular theoretical method depends upon the atomic system under study. The problem is essentially one of producing accurate wavefunctions by numerical means so that transition matrix elements can be computed. Moreover, the wavefunctions of the two states must be comparably accurate. For example, in systems like Li, Na, K, Mg^+, Ca^+, which have single electrons outside a closed shell, it is possible to compute quite good wavefunctions using a semi-empirical potential that is based upon a central, screened Coulomb potential plus the effects of the polarization of the core electrons by the valence electron. As long as the matrix elements are not too small, f-values accurate to better than 10% can be calculated this way. Small matrix elements mean large cancellation effects between the wavefunctions and sensitivity to fine effects: more complicated methods are then required to give accurate results. In systems with more than one electron in an open shell, the most elaborate theoretical methods are usually necessary. As a general rule, configuration interaction computations provide the most reliable results, and in the hands of the most careful users provide accuracy comparable to that of a good experimental determination. One criterion for estimating the worth of a theoretical result is how well the wave functions reproduce the measured energy levels.

(ii) Experimental methods

There are basically two methods, with many variations:

Lifetime measurements. Lifetimes of excited states can be measured quite accurately. Because $\tau_i = (\sum_j A_{ij})^{-1}$ is related to a sum of transition probabilities, it does not necessarily directly give the A_{ij} value for any particular transition. Since the measurement is basically one of intensity as a function of time, the intensity of light emerging in some transition can depend not only on the lifetime of the upper state, but also the rate at which it is being populated by cascades from higher states.

Absorption measurements. The amount of light absorbed in a particular line by a *known* number of absorbing atoms is directly related to the oscillator strength. The usual difficulty lies in determining the number of absorbers accurately.

5. Example

C II $1s^2 2s^2 2p\ ^2P^o - 1s^2 2s 2p^2\ ^2D$ multiplet

Here, the electron configurations are $1s^2 2s^2 2p$ (the lower state) and $1s^2 2s 2p^2$ (the upper state), while the spectroscopic terms are the doublet P and doublet D. The superscript ^{o} in the lower state means the parity is odd, where the parity is defined as Σl_i, where the summation runs over all electrons.

For example: $^2P^o$ term $1s^2$ 2x0=0 l=0
$2s^2$ 2x0=0 l=0
2p 1x1=1 l=1
$\sum_i l_i$=1 (an *odd* number, so the parity is odd)

$^2D^o$ term $1s^2$ 2x0=0 l=0
$2s^2$ 1x0=0 l=0
2p 2x1=2 l=0
$\sum_i l_i$=2 (an *even* number, so the parity is even)

The $^2P^0$ term has $S = 1/2$ ($2S + 1 = 2$) and $L = 1$, thus the resultant total angular momentum J can have values $1 \pm 1/2$, that is, J=1/2, 3/2. The $^2D^{(e)}$ term has $S = 1/2$ ($2S + 1 = 2$) and $L = 2$, thus J=3/2 and 5/2 occur.

The possible radiative transitions between levels of these two multiplets are the following "lines":

$^2P^o_J - ^2D_J$	λ_{vac}	f	$\sum_l A_{ul}(s^{-1})$
J=1/2 − 3/2	1334.5323Å	0.129	2.90×10^8
J=3/2 − 5/2	1335.7077Å	0.116	2.88×10^8
J=3/2 − 3/2	1335.6627Å	0.0128	2.90×10^9

From here, we can work backwards to the energy levels, taking the ground level $^2P^o_{1/2}$ as 0.00. The first and 3rd lines have a common upper state, so the wavelength difference gives the fine-structure, $J = 1/2 - 3/2$, splitting of the ground term, $1/\lambda_1 - 1/\lambda_3$=63.417 cm^{-1} Given this, the fine-structure, $J = 3/2 - 5/2$, splitting of the upper term follows from the wavelength difference of lines 2 and 3: 2.522 cm^{-1}. Thus, the so-called term energies work out to be:

Term	J	$E(\mathrm{cm}^{-1})$
$^2\mathrm{P}^o$	1/2	0.000
	3/2	63.417
$^2\mathrm{D}$	3/2	74,932.619
	5/2	74,930.096

Notice that the level of higher multiplicity in ^{2}D actually lies lower in energy in this case.

The mean term energies $\propto \sum_J (2J+1)E_J$ are $^2\mathrm{P}^o$: 42.278 cm^{-1}
^{2}D : 74,931.105 cm^{-1}

and the mean multiplet wavelength is λ_M=1335.313 Å.

Individual A-values can be computed from the listed f:

line 1: $(2J_a+1)=4 \quad (2J_b+1)=2 \Rightarrow A_{ab} = 2.416 \times 10^8$ s^{-1}
line 2 $A_{ab} = 2.891 \times 10^8$ s^{-1}
line 3 $A_{ab} = 4.79 \times 10^7$ s^{-1}

Note that the *total* $\sum_b A_{ab}$ for the $^2\mathrm{D}_{3/2}$ state is:

$A_{tot} = (2.416 + 0.479) \times 10^8 = 2.895 \times 10^8$ s^{-1}

while that for $^3\mathrm{D}_{5/2}$ is just:

$A_{tot} = 2.891 \times 10^8$ s^{-1}.

Note also that $\sum_a f_{ab} = 0.129$ for $^2\mathrm{P}^o_{1/2}$
and $= 0.129$ for $^2\mathrm{P}^o_{3/2}$.

6. Intercombination transitions

In pure LS coupling, radiative transitions between states with different total spin S are forbidden. However, because of the spin-orbit interaction, these so-called intercombination transitions can occur weakly. Since the spin-orbit coupling increases rapidly with increasing Z, the intensities of the intercombination lines behave similarly. For example, intercombination transitions are practically absent in the He spectrum, but in the Hg spectrum the line at 2537 Å ($6s^2 - 6s6p\ ^3\mathrm{P}_1$) is very intense.

The matrix elements of the various multipole moments for intercombination transitions can be expressed within pure LS coupling by taking the appropriate linear combinations due to spin-orbit interaction. The rigorous selection rules given earlier apply. Intercombination lines are sometimes called "semi-forbidden" lines, and are indicated by a bracket on the right-hand side, for example, the C III] $2s^2\ ^1\mathrm{S} - 2s2p\ ^3\mathrm{P}$ lines at λ1906, 1908 Å. Such lines can be very prominent in the spectra of planetary nebulae or other high temperature nebulae, some of the more important transitions are summarized in Tables 3.1 and 3.2.

7. Two-photon emission

Levels such as the $2\ ^2\mathrm{S}_{1/2}$ level of H and the $2\ ^1\mathrm{S}_0$ level of He are called "metastable" because in the usual approximations, they cannot decay by electric dipole, electric quadrupole, or magnetic dipole radiation according to the $J_a = 0 \rightarrow J_b = 0$ rule. However, the levels can decay by simultaneous emission of *two* photons:

$$\mathrm{H(2s)} \rightarrow \mathrm{H(1s)} + \mathrm{h}\nu_1 + \mathrm{h}\nu_2. \qquad (3.48)$$

Table 3.1– Intercombination Transition Probabilities for He-like Ions

Transition Ion	$W(1^1S_0 - 2^3P_1)$, $[s^{-1}]$	$W(2^1S_0 - 2^3P_1)$, $[s^{-1}]$	$W(2^3S_1 - 2^1P_1)$, $[s^{-1}]$
He I	1.80×10^2	0.027	1.55
Li II	1.81×10^4	0.057	4.18×10^1
Be III	4.01×10^5	0.052	3.83×10^2
B IV	4.23×10^6	0.016	2.05×10^3
C V	2.84×10^7	6×10^{-7}	7.87×10^3
N VI	1.40×10^8	0.018	2.43×10^4
O VII	5.53×10^8	0.25	6.41×10^4
F VIII	1.85×10^9	1.36	1.50×10^5
Ne IX	5.43×10^9	4.96	3.20×10^5

Table 3.2– $2^1S_0 - 2^3P_1$ Transition Probability in Be-like Ions, $W[s^{-1}]$

Be I	B II	C III	N IV	O V	F VI
0.71	2.0×10^1	1.9×10^2	9.2×10^2	3.6×10^3	1.1×10^4
Ne VII	Na VIII	Mg IX	Al X	Si XI	P XII
2.9×10^4	7.3×10^4	1.6×10^5	3.3×10^5	6.5×10^5	1.1×10^6
S XIII	Cl XIV	Ar XV	K XVI	Ca XVII	
2.1×10^6	3.2×10^6	5.2×10^6	8.2×10^6	1.3×10^7	

The probability for simultaneous emission of two photons with one in the range ν_1 to $\nu_1 + d\nu$ in, for example, the case of He is:

$$A(\nu_1)d\nu_1 = \frac{2^{10}\pi^6 e^4}{h^2 c^6}\nu_1^3\nu_2^3 \times$$

$$\left\langle \left| \sum_{n'} \left[\frac{< 1^1S|\vec{d}\cdot\vec{\epsilon}_1|n' >< n'|\vec{d}\cdot\vec{\epsilon}_2|2^1S >}{\nu_{n'2} + \nu_2} + \right. \right. \right.$$

$$\left. \left. \left. \frac{< 1^1S|\vec{d}\cdot\vec{\epsilon}_2|n' >< n'|\vec{d}\cdot\vec{\epsilon}_1|2^1S >}{\nu_{n'2} + \nu_1} \right] \right| \right\rangle_{av}$$

where the summation extends over *all* triply degenerate $n'\ ^1P_1 \rightarrow 2\ ^1S_0$, $\nu_2 = \frac{E(^1S_0)}{h} - \nu_1$, and the average is over the polarization directions $\vec{\epsilon}_1$, $\vec{\epsilon}_2$. Physically, the two-photon process occurs by weak coupling to all of the (higher) intermediate P states. See, for example, Jacobs 1971, *Phys. Rev. A* **4**, 939 Drake *et al* 1960, *Phys. Rev.* **180**, 25 for more details.

The total two-photon emission probability A_{total} is $8.23\ s^{-1}$ for the H $2\ ^2S_{1/2}$ level and $51.3\ s^{-1}$ for the He $2\ ^1S_0$ level. The photons emerge with a broad probability distribution subject to the constraint that the sum of the photon energies $h\nu_1 + h\nu_2 = E_{2s} - E_{1s}$. The spectra for H and He are illustrated in Figures 3.1 and 3.2, respectively.

The continuous emission from H($2\ ^2S_{1/2}$) is observed in the spectra of low-density ionized nebulae in which the $2\ ^2S_{1/2}$ level is populated by recombination and cascade from higher levels, and has a good chance of radiating two photons before undergoing a collision or another photo-ionization. The resulting spectra of both H and He can be

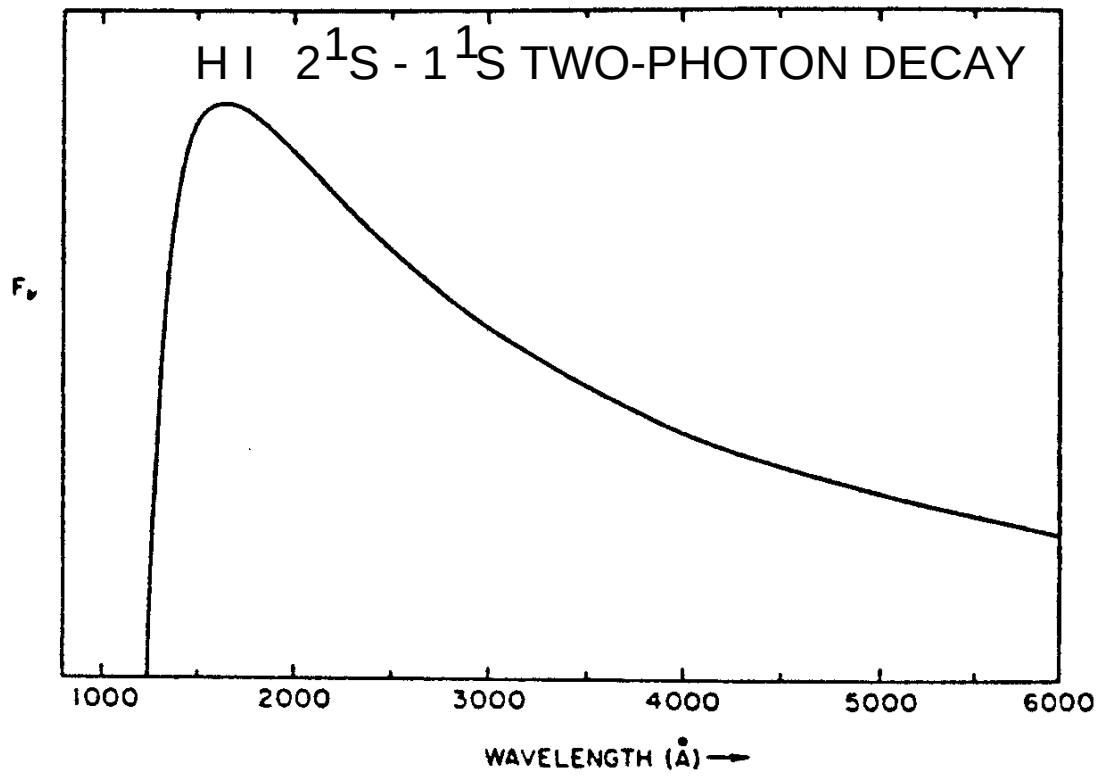

Figure 3.1– The relative emissivity (in ergs/s/Hz) due to the two-photon 2s-1s decay in hydrogen.

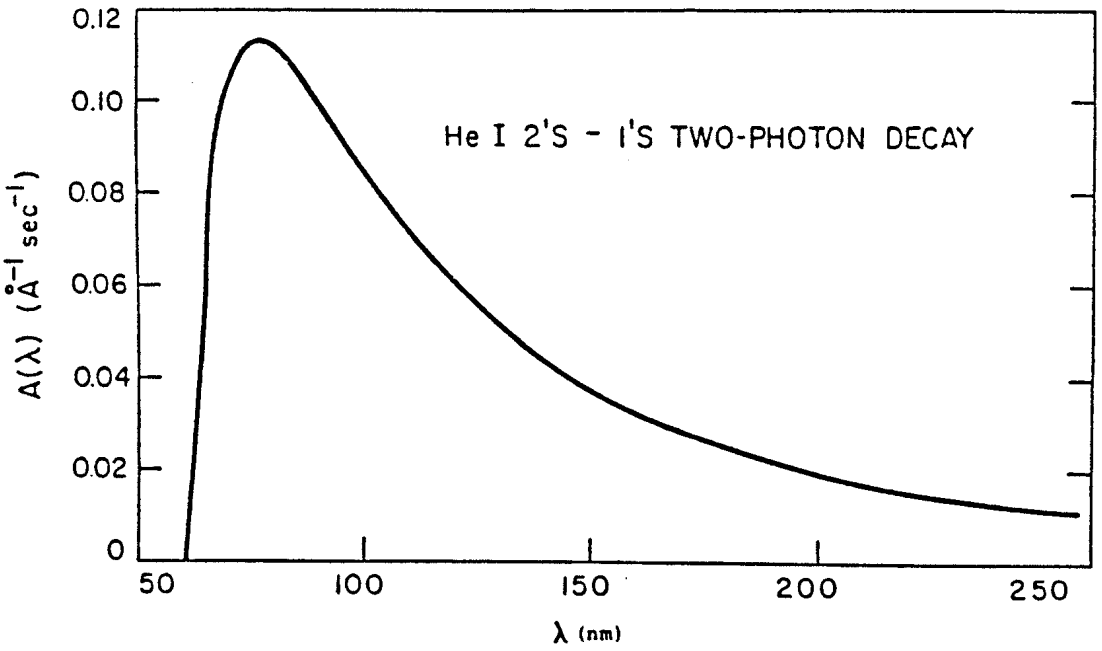

Figure 3.2– Two-photon decay spectrum of the 2^1S state of helium (w/wavelength λ in nm).

important sources of photons inside nebulae. For more details, see for example, Spitzer and Greenstein (1951, *Ap. J.* **114**, 407 and Gaskell (1980, *Observatory* **100**, 148).

The He ($2\ ^3S_1$) state is also highly metastable. However, its dominant form of radiation decay is by direct magnetic dipole transitions to the ground state, with $A(2\ ^3S - 1\ ^1S) = 1.27 \times 10^{-4}\ s^{-1}$ (Drake 1971, *Phys. Rev.* **A3**, 908). The transitions can occur weakly if exact spin functions are used. This means that in relatively low-density plasmas where He ($2\ ^3S$) can be populated by recombination, this state can be significantly populated and can behave like a quasi-ground state of triplet He atoms (see, for example, Drake and Robbins 1972, *Ap. J.* **171**, 55).

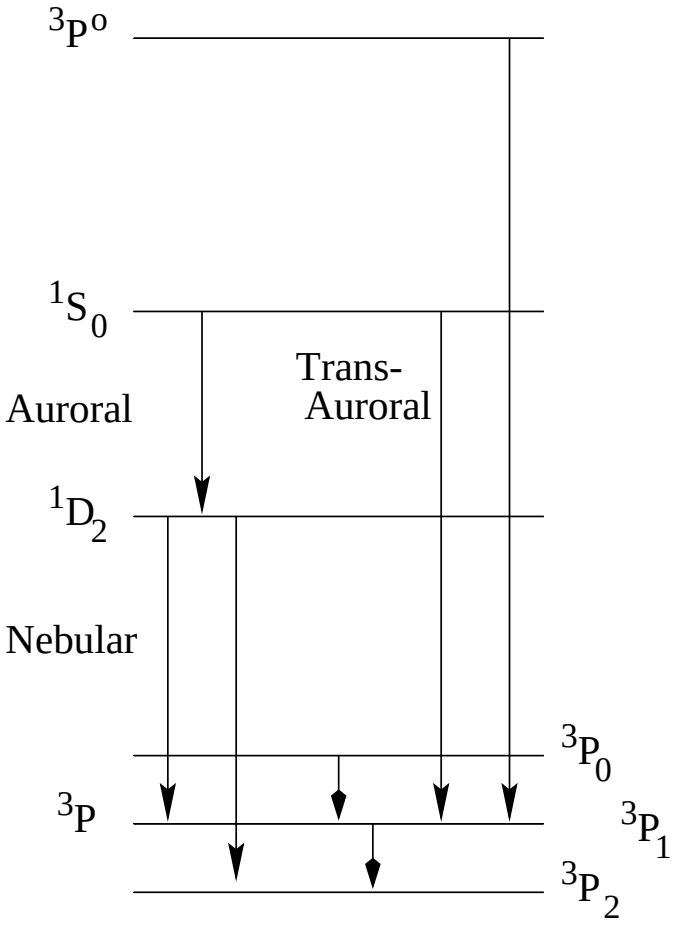

8. One more example

Consider the oxygen atom with ground state configuration $1s^2 2s^2 2p^4$. As we have seen, this configuration gives rise to the terms $^3P_{2,1,0}$,$^1D_2$, and $^1S_0$. The splitting between the lowest two terms is 15,790 cm $^{-1}$ (1.96 eV) and between the highest two terms is 17,925 cm^{-1} (2.22 eV), so that the transitions occur at visible wavelengths, λ 6331 and 5577 Å, respectively. The excited terms correspond to configurations $2p^3ns$, $2p^3np$, $2s2p^5$, etc.... The excitation energy of the lowest excited (triplet) term is 76,717 cm^{-1} or 9.51eV, so that the resonance transition lies at vacuum ultraviolet wavelengths, 1302 Å.

For historical reasons, transitions between the middle and lowest terms are called "nebular-type" transitions (for oxygen: $^1D - ^3P$) and those between the highest and middle

terms are called "auroral-type" transitions. The strong green line in the Earth's aurora, λ 5577 [O I], is from $^1S_0$ to $^1D_2$. Forbidden lines are indicated by square brackets. Transitions from the top to the lowest term are called "trans-auroral" transitions. Transitions between individual levels of a ground configuration, such as $^3P_2 - ^3P_1$, are called "fine-structure" transitions. These lie typically at far-infrared or submillimeter wavelengths and are observed in dense, cold interstellar clouds. For example, for oxygen $^3P_1 \rightarrow ^3P_2$ occurs at 63 μm and $^3P_0 \rightarrow ^3P_1$ at 145 μm.

Both the nebular, auroral and transauroral transitions are electric dipole forbidden. However, the $^1D_2 - ^3P_{1,2}$ and the $^1S_0 - ^3P_1$ transitions can occur as magnetic dipole transitions. Both the $^1S_0 - ^1D_2$ and $^1S_0 - ^3P_2$ transitions clearly require electric quadrupole radiation, since $\Delta J = 2$. The transition probabilities for these transitions are quite low, typically A =0.01 s^{-1}, so that the lifetime of the state can be as large as 100 sec. More specifically, for oxygen:

$$^1D_2 - ^3P_0 : A = 7.23 \times 10^{-7} \text{ s}^{-1}$$
$$^1D_2 - ^3P_1 : A = 2.11 \times 10^{-3} \text{ s}^{-1}$$
$$^1D_2 - ^3P_2 : A = 6.34 \times 10^{-3} \text{ s}^{-1}$$

$$^1S_0 - ^3P_1 : A = 7.32 \times 10^{-2} \text{ s}^{-1}$$
$$^1S_0 - ^3P_2 : A = 2.88 \times 10^{-4} \text{ s}^{-1}$$

$$^1S_0 - ^1D_2 : A = 1.22 \text{ s}^{-1}$$

$$^3P_0 - ^3P_1 : A = 1.74 \times 10^{-5} \text{ s}^{-1}$$
$$^3P_1 - ^3P_2 : A = 8.92 \times 10^{-5} \text{ s}^{-1}$$

IV. PHOTOIONIZATION AND RECOMBINATION

A. Photoionization

1. Hydrogen

Consider a transition in an atom from a bound state nl to a continuum state kl in which one electron is free. This is usually called a "bound-free" transition. This can result upon absorption of a photon of energy $h\nu \geq I_n$, the ionization potential of the atom in state n. The probability of this absorption as a function of photon frequency ν is described in terms of a cross section:

$$\sigma_n(\nu) \quad = \quad \frac{8\pi^3\nu}{3c} \cdot \frac{1}{g_n} \sum_{l'=l\pm1} \mid \int \Psi^*_{kl'} \; \vec{d} \; \Psi_{nl} d\tau \mid^2 \qquad [\mathrm{cm}^2] \tag{4.1}$$

where g_n is the degeneracy of level n and the integration extends over all coordinates and includes a sum over all possible continua. The Ψ_{kl} are continuum eigenfunctions belonging to eigenvalues $E = (I_n + h\nu)$, and the energy normalization is given by:

$$< \Phi | \Phi >= \int a(E) a^*(E) \Psi_{kl} \Psi^*_{kl}(E) dE = 1 \tag{4.2}$$

such that $|a(E)|^2 dE$ gives the probability of finding the system (ion plus free electron) in the interval $(E, E + dE)$.

For H atoms, the cross section can be computed exactly (see e.g. Sobelman Ch. 9.5):

$$\sigma_H \quad = \quad 3.4439 \times 10^{-16} \left(\frac{\nu_1}{\nu}\right)^4 \frac{e^{-[(4\mathrm{arctan}\epsilon)/\epsilon]}}{1 - e^{-2\pi/\epsilon}} \qquad [\mathrm{cm}^2] \tag{4.3}$$

where $\epsilon = (\nu - \nu_1)^{1/2}$ and $\nu_1 = 109{,}678.77$ cm^{-1}. At the ionization threshold, $\sigma_H(\nu_1) = 6.308 \times 10^{-18}$ cm^2. Note that for a pure Coulomb potential (i.e. a strictly hydrogenic system), the photoionization cross section is finite at threshold. Table 4.1 lists the cross sections at various wavelengths.

Table 4.1– Photoionization cross sections in cm^2 for the ground state of H

λ(Å)	$\sigma_H(\lambda)$
912	6.3(-18) (meaning 6.3×10^{-18})
760	3.9(-18)
651	2.9(-18)
570	1.8(-18)
456	9.3(-19)
304	2.9(-19)
182	6.3(-20)
91.2	7.4(-21)
45.6	8.2(-22)
22.8	8.6(-23)
9.12	4.1(-24)

For a hydrogenic system of charge Z initially in state of principal quantum number n, the cross section is often written in terms of a Gaunt factor g_{in} for ionization, which is of order unity:

$$\sigma(\nu) \;=\; g_{in}\frac{32\pi^5 e^6}{3^{3/2}h^3\nu^3}\cdot\frac{\mathrm{R}Z^4}{n^5} \tag{4.4}$$

where R is the appropriate Rydberg constant $\mathrm{R}=\mathrm{R}_\infty/(1+m_e/M)$. The Gaunt factor is the correction factor for the quantum result with respect to the classical treatment. For H,

$$\sigma(\nu) \;=\; 2.814\times10^{29}\nu^{-3}n^{-5}g_{in} \qquad [\mathrm{cm}^2] \tag{4.5}$$

and specifically for H in its ground level, to an excellent approximation

$$\sigma(\nu) \;\approx\; 6.3\times10^{-18}\left(\frac{\nu_1}{\nu}\right)^3 \qquad [\mathrm{cm}^2] \quad . \tag{4.6}$$

The classic paper on radiative properties of hydrogenic systems is by Karzas and Latter 1961, *Ap. J. Suppl.*, **6**, 167.

Often, photoionization cross sections are represented in the form

$$\sigma(E) \;=\; \sigma(I)\left\{\alpha\left(\frac{I}{E}\right)^S \;+\; (1-\alpha)\left(\frac{I}{E}\right)^{S+1}\right\} \quad , \tag{4.7}$$

where $\sigma(I)$ is the threshold cross section at the ionization potential I. For H, a fit to within 10% for $E<2$ keV is obtained with α=1.8 and $S=3.2$. For higher photon energies, an accurate representation is provided by the limiting form:

$$\sigma_H(E) \;\approx\; 4.1\times10^{-17}(I/E)^{7/2} \quad \mathrm{cm}^2. \tag{4.8}$$

In some astrophysical plasmas, the metastable $2\ ^2\mathrm{S}_{1/2}$ state of H may be sufficiently populated that absorption from it is a significant source of opacity. The calculated cross sections for this state are listed in Table 4.2

Table 4.2– Photoionization cross sections (in cm^2) for the metastable $2\ ^2\mathrm{S}_{1/2}$ state of H

λ(Å)	3647	2763	1600	1024	418	170	86.9
$\sigma(\mathrm{cm}^2)$	3.7(-18)	2.0(-18)	5.9(-19)	5.0(-20)	9.4(-21)	1.4(-21)	1.9(-22)

2. Helium

a) direct photoionization

The cosmic abundance of helium with respect to hydrogen is about 0.1. Helium can be photoionized by absorption of photons with energies greater than 24.58 eV or wavelengths shorter than 504 Å. Thus, the production of He^+ requires a more energetic, hotter light source than does the production of H^+.

Exact calculations are no longer possible for He, but highly accurate calculations can be performed which agree well with experiments. Table 4.3 lists values of the photoionization cross sectoin from the ground state of helium, $\sigma_{He}(E)$, for several

wavelengths. They can be represented approximately by equation (4.7) with the parameters $\sigma_{He}(I) = 7.6 \times 10^{-18}$ cm^2, $\alpha = 2.7$ and $S = 2.83$.

Table 4.3– Photoionization cross-sections [cm^2] for the He ground state

λ(Å)	504	413	310	207	155
σ(cm^2)	7.4(-18)	5.4(-18)	3.2(-18)	1.4(-18)	8.1(-19)

As Table 4.4 shows, the ratio of the photoionization cross sections of helium to hydrogen increases rapidly toward shorter wavelengths:

Table 4.4– Ratio of He to H photoionization cross sections

λ(Å)	504	413	310	207	155
σ(He)/σ(H)	6.3	8.1	11.0	15.9	20.4

The high energy limit for helium

$$\sigma_{He}(E) \;=\; 2.5 \times 10^{-15} (I_H/E)^{7/2} \qquad [\mathrm{cm}^2] \tag{4.9}$$

is about 60 times larger than for hydrogen. Hence, in a cosmic abundance gas, helium is a more efficient absorber of short wavelength photons than is atomic hydrogen.

Photoionization of the 2 ^{3}S$_1$ state of helium has a threshold at 2598 Å. It may contribute to the opacity in dense nebulae, and is an additional source of free electrons.

b) autoionization

The excitation energy of the He 2 ^{3}S state is 19.8 eV. Thus, this state, in which only one electron is excited out of the 1s orbital, already lies more than halfway toward the ionization threshold of 24.6 eV. This suggests immediately that "doubly-excited" states, belonging to configurations $(nl, n'l')$ ^1L, ^3L with $n \geq 2, n' \geq 2$ are likely to have energies larger than that needed to remove one electron completely. Such configurations make perfectly good, well-defined stationary states; however, because they are embedded within the continuum of He$^+$ plus free electron states, these doubly-excited states have high probabilities of undergoing transitions. They can either radiate to low-lying He states below the ionization threshold, or they can decay "non-radiatively" into the continuum states:

$$\mathrm{He}(n, l, n'l') \rightarrow \mathrm{He}^+ + e(\epsilon) \tag{4.10}$$

in a process called "auto-ionization". Experimentally, these states show up as "resonances" in the photon absorption cross-section of He in the EUV. The interaction between a discrete state and a continuum results in a cross section profile that looks like:

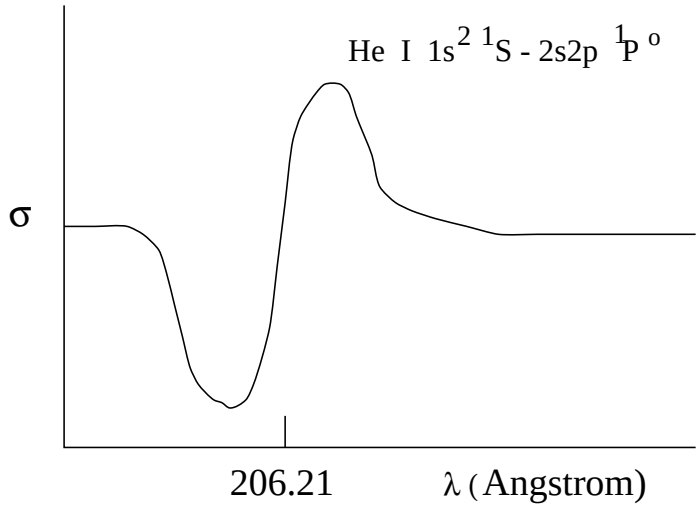

This is called a Fano-profile, and can be written as:

$$\sigma(E) \;=\; \sigma_b(E)\frac{(q+\epsilon_{res})^2}{1+\epsilon_{res}^2} \tag{4.11}$$

where $\sigma_b(E)$ is the smooth background cross section, $\epsilon_{res} = 2(E - E_a)/\Gamma_a$, $\Gamma_a = \hbar/\tau_a$ is the autoionizing width, and q is the so-called "shape" parameter (see Fano 1961, *Phys. Rev.* **124**, 1866.) Fig. 4.1 illustrates the resonance structure of the photoionization cross section of He, whereas Fig. 4.2 shows the location of some of the He doubly-excited states.

Photoionization of ground state helium is not much enhanced by absorption into the resonances because they involve weak two-electron transitions from the $(1s)^2$ ^{1}S state, but photoionization of the metastable atoms can be increased considerably for photons with energies near the resonance energies.

The classic paper on the He autoionizing resonances is that of Madden and Codling (1965, **Ap. J. 141**, 364). In more complex multi-electron systems, states of multiply-excited configurations need not lie above the first ionization limits.

Autoionizing resonances do sometimes appear in astronomy: a good example is an absorption feature in the solar spectrum near λ 1932.0, 1936.4 Å that is due to a transition from the ground state to an autoionizing resonance in Al I ($3s^2 3p\ ^2P^o$ - $3s3p^2\ ^2S_{1/2}$). (See Kohl and Parkinson 1973, *Ap. J.* **184**, 641).

3. Other elements

Although elements heavier than H and He have small abundances relative to H, lines of their ions show up prominently in the spectra of nebulae. As for He, no exact results can be obtained for their photoionization cross sections, but accurate calculations are possible for most low Z atoms.

For atoms with an open shell configuration, removal of an electron may lead to more than one final state. For example, removal of an outer valence 2p electron from the ground state of O ^{3}P ($1s^2 2s^2 2p^4$) can produce an oxygen ion with the configuration $1s^2 2s^2 2p^3$ in any one of the ground ^{4}S and metastable ^{2}D and ^{2}P states.

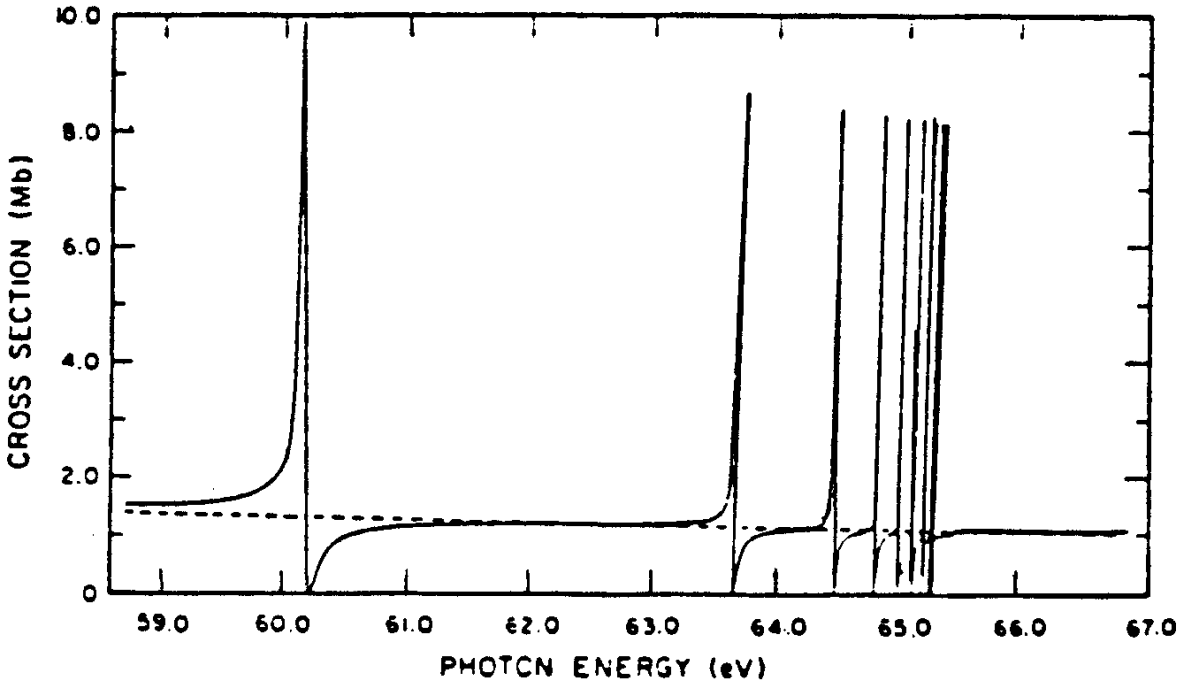

Figure 4.1: He photoabsorption cross section as a function of photon energy. The structures arise from absorption into a $^1P^o$ series of resonances.

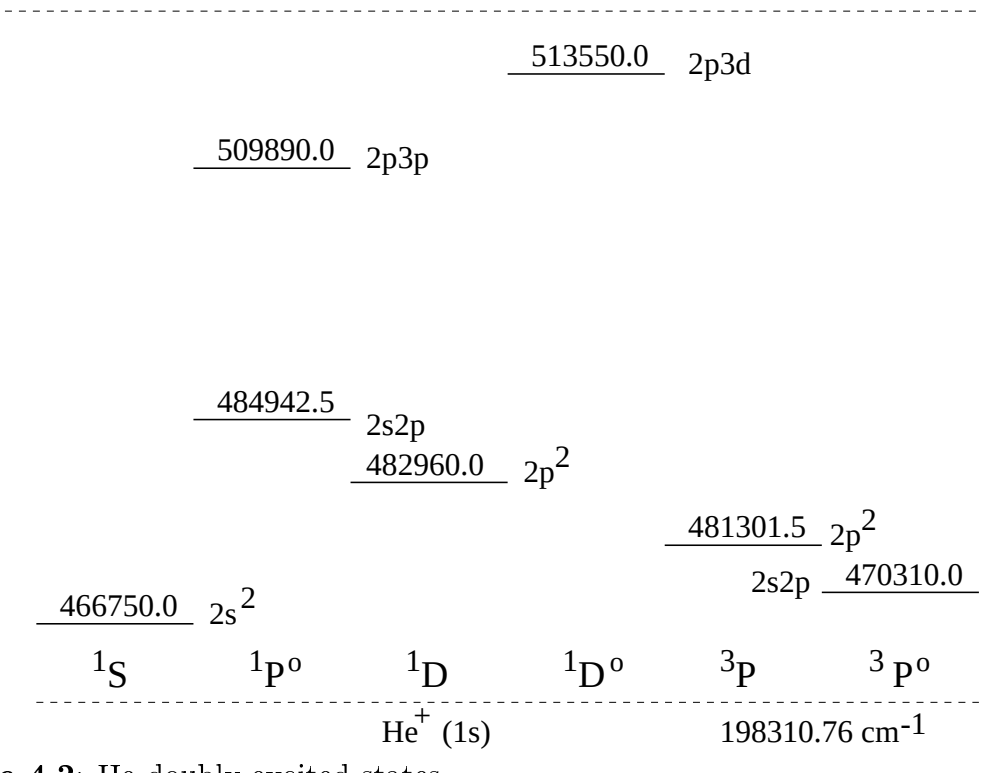

Figure 4.2: He doubly-excited states.

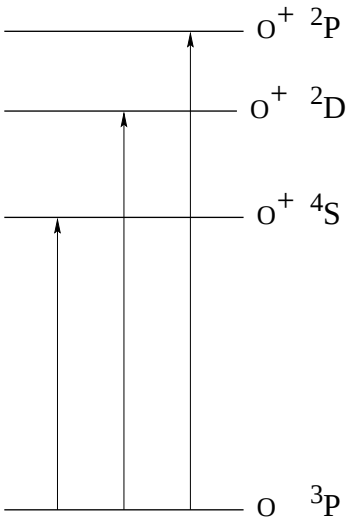

The ionization thresholds are 13.6 eV, 16.6 eV and 18.6 eV, respectively. Table 4.5 lists approximate values for the different "channels." The smooth behavior of the cross section in Table 4.5 is interrupted between the $O^+(^4S)$ and $O^+(^2D)$ thresholds by a series of resonances with configurations $(2p^3ns)\ ^3D$, $(2p^3nd)\ ^3D$ and $(2p^3nd)\ ^3S$, converging to $O^+\ ^2D$. More series of resonances occur below the $O^+\ (^2P)$ threshold. Thus, the cross section will have the general appearance:

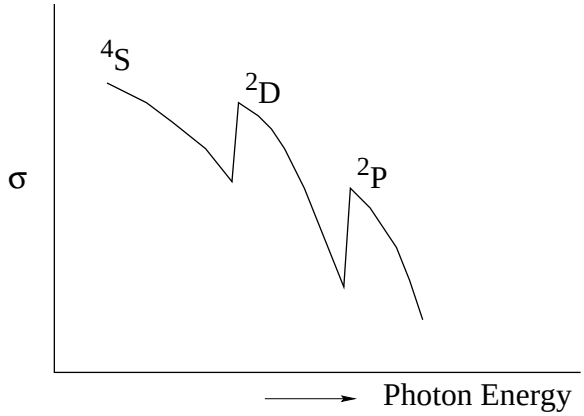

with small resonances superimposed in addition.

Table 4.5– Photoionization cross sections of oxygen in 10^{-18} cm^2

λ(Å)	$O^+(^4S)$	$O^+(^2D)$	$O^+(^2P)$
910	4.18		
800	4.76	–	
730	3.88	4.77	–
670	3.80	5.33	2.76
600	3.63	5.51	3.07
500	3.33	5.31	3.17
400	2.90	4.60	2.85
300	2.42	3.58	2.28
200	1.76	2.25	1.47

Table 4.6– Parameters in the Cross Section Formula

$$\sigma(E) = \sigma(I)\left\{\alpha\left(\frac{I}{E}\right)^{S} + (1-\alpha)\left(\frac{I}{E}\right)^{S+1}\right\}$$

species	final state	s	α	σ(I) (10^{-18} cm^2)
C	$C^+(^2P)$	2.0	3.317	12.2
C^+	$C^{2+}(^1S)$	1.5	2.789	10.3
N	$N^+(^3P)$	2.0	4.287	11.4
N^+	$N^{2+}(^2P)$	3.0	2.860	6.65
N^{2+}	$N^{3+}(^1S)$	3.0	1.626	2.06
O	$O^+(^4S)$	1.0	2.661	2.94
	$O^+(^2D)$	1.5	4.378	3.85
	$O^+(^2P)$	1.5	4.311	2.26
O^+	$O^{2+}(^3P)$	2.5	3.837	7.32
O^{2+}	$O^{3+}(^2P)$	3.0	2.014	3.65
O^{3+}	$O^{4+}(^1S)$	3.0	0.831	1.27
Ne	$Ne^+(^2P)$	1.0	3.769	5.35
Ne^+	$Ne^{2+}(^3P)$	1.5	2.717	4.16
	$Ne^{2+}(^1D)$	1.5	2.148	2.71
	$Ne^{2+}(^1S)$	1.5	2.126	0.52
Ne^{2+}	$Ne^{3+}(^4S)$	2.0	2.346	1.80
	$Ne^{3+}(^2P)$	2.5	2.225	2.50
	$Ne^{3+}(^2D)$	2.5	2.074	1.48
Ne^{3+}	$Ne^{4+}(^3P)$	3.0	1.963	3.11
Ne^{4+}	$Ne^{5+}(^2P)$	3.0	1.47	1.40
Ne^{5+}	$Ne^{6+}(^1S)$	3.0	1.145	0.49

from: Dalgarno, A. Harvard University Astronomy 209

There is a large body of data on photoionization cross sections, both experimental and theoretical. Mendoza's (1983) review, referred to earlier, also contains references to many photoionization processes of astrophysical interest. For a uniform, but not as accurate set of cross sections for a large number of ions at energies that extend into the X-ray region, see Reilman and Manson (1980, *Ap. J. Suppl.* **40**, 815: 1981 *Ap. J. Suppl.* **46**, 115; 1986 *Ap. J. Suppl.* **62**, 939).

Table 4.6 reproduces the parameters in the fit to Equation (4.7) for ions of C, N, O and Ne. New results with improved accuracy appear regularly.

Note: recall the oscillator strength sum rule formula

$$\frac{\pi e^2}{m_e c} f \;=\; \int \sigma d\nu \tag{4.12}$$

for bound-bound transitions; this suggests that it is possible to describe the probability of continuous absorption in terms of a differential oscillator strength:

$$\frac{df}{d\epsilon} \;=\; \frac{df}{h d\nu} \;=\; \frac{m_e c}{\pi e^2 h}\,\sigma \quad . \tag{4.13}$$

4. Inner shell ionizations

So far, we have considered only the removal of a valence electron. If the photon energy is sufficiently high, an electron in an inner shell can be removed directly. This normally requires X-ray or γ-ray photons (such as from a supernova remnant). The inner shells are designated as:

n	l	j	shell
1	0	1/2	K
2	0	1/2	L_I
2	1	1/2	L_{II}
2	1	3/2	L_{III}
3	0	1/2	M_I
3	1	1/2	M_{II}
3	1	3/2	M_{III}
3	2	3/2	M_{IV}
3	2	5/2	M_V

What happens following the creation of a "vacancy" in an inner shell of an atom or ion? Clearly, the system is in a state of very high excitation. Several outcomes are possible depending upon the initial number of electrons in the system, the shell with the initial vacancy, and so on (Figure 4.3 graphically illustrates these various processes):

1) An electron from the valence shell or a higher inner shell can fill the vacancy by an allowed radiative transition. Usually a very energetic photon is involved and this is a way of producing X-ray line spectra (Radiative decay). The probability that a vacancy is filled by a radiative transition is called the "fluorescence yield", and is conventionally denoted by ω_K for the K-shell.

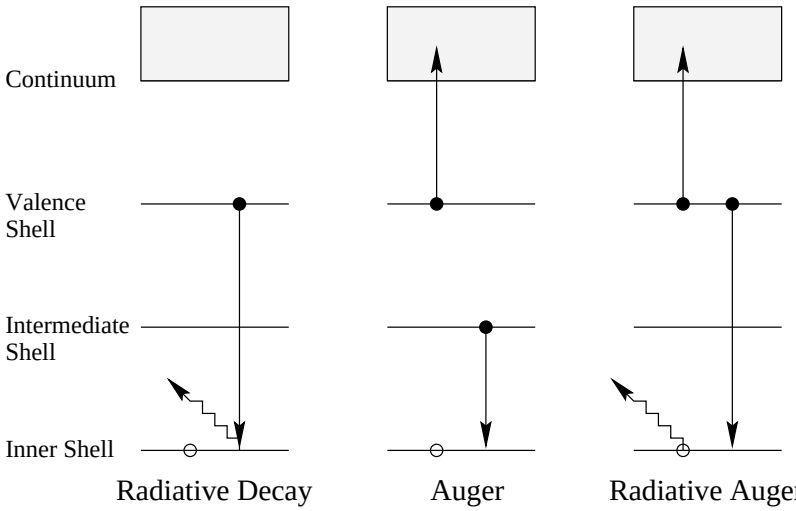

Figure 4.3– Schematic diagram illustrating the various possible processes following inner shell ionization.

2) An intermediate-shell electron can fill the inner shell vacancy with the simultaneous ejection of an outer electron to carry off the transition energy and to conserve angular momentum (Radiationless Auger effect). Note that this is a gratuitous ionization: two electrons have been liberated for the price of one. In complex atoms, more than one Auger electron can be produced in the cascade of transitions to fill inner shell vacancies in so-called "shake-off" processes. These multiple ionization events complicate the equation of ionization equilibrium by coupling together ions of widely different charge states.

3) Another variant is possible in which the outer shell electron fills the inner shell vacancy and the excess energy is carried off partly by another liberated valence electron, and partly by emission of a photon (Radiative Auger effect).

Table 4.7– Number of Auger electrons emitted.

initial subshell	Number of initial electrons in atom/ion					
vacancy	4-10	11	12	13	14	15-18
2p	0	0	1	1	1	1
2s	0	1	1	2	2	2
1s	1	1-2	2-3	2-3	3	3-4

The selection rules for an Auger transition are $\Delta L = \Delta\ S = \Delta J = 0$, and no parity change, and so overall behavior of the photoionization cross section of an atom has the general appearnce outlined below.

Consider again the case of oxygen as an example. Resonances appear in the absorption cross section at high photon energies, in which the inner shell 2s electron is excited to autoionizing states of ^{3}S, ^{3}P and ^{3}D symmetries with configurations ($2s2p^4np$), converging to the ^{4}P and ^{2}P O^+ ($1s^2 2s2p^4$) states at 435 and 310 Å, respectively. The cross sections for this L_I ionization process are typically 10^{-18} cm^2 around threshold. However, as Table 4.7 shows, removal of a 2s electron does not yet lead to Auger electrons for oxygen. Thus,

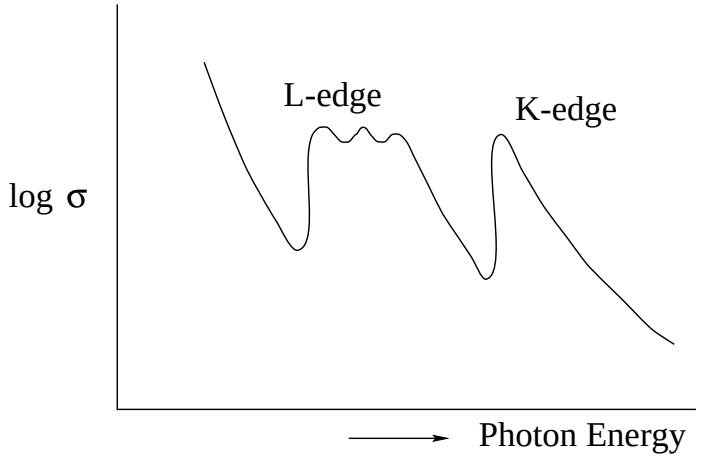

the O^+ states will decay by fluorescence. The ^4P ($2s2p^4$) state of O^+ decays principally to the $^4S^o$ ($2s^22p^3$) state emitting a photon at 843 Å, and the ^2P ($2s2p^4$) state decays to the $^2D^o$ ($2s^22p^3$) and $^2P^o$($2s^22p^3$) states through photons at 504 and 534 Å respectively.

The 1s electron of oxygen can be removed at E>545eV or λ <22.75 Å, leading to ^4P and ^2P states of O^+:

$$O\ ^3P\ (1s^22s^22p^4) + h\nu \rightarrow O^+\ (1s2s^22p^4)\ ^{4,2}P + e \tag{4.14}$$

The cross sections for this K-shell ionization are given in Table 4.8.

Table 4.8– K-shell photoionization cross sections for O in 10^{-18}cm^2.

λ(Å)	20.7	10.3	5.2	2.5
σ(cm^2)	0.44	0.075	0.011	0.001

Radiative decay of the excited state created by the K-shell vacancy leads to a pair of emission lines labelled K_{α_1} and K_{α_2}, corresponding respectively to the $2p_{1/2}$ - $1s_{1/2}$ and $2p_{3/2}$ - $1s_{1/2}$ transitions. However, for light elements such as oxygen, the radiationless Auger process is much more probable:

$$O^{+}\ (1s2s^22p^4) \rightarrow O^{2+}\ (1s^22s^22p^2) + e \tag{4.15}$$

In this case, it is called a K-LL transition, because a K-shell vacancy is created, the vacancy is filled by an L-shell electron and a second L-shell electron is ejected.

For neutral, light atoms with $Z < 10$, the K-shell fluorescence yields are measured to be small, ω_K <0.02, and calculations suggest that it is less than a factor of three higher for positive ions. Radiative Auger yields are computed to be ω_k^{RA} <0.01ω_K. Thus, the probability of a radiationless Auger transition to fill an inner shell vacancy is nearly unity. For heavy elements, iron has ω_K=0.35, while for nickel ω_K=0.38.

The K-shell ionization cross sections of an element change little as the outer electrons are removed, except for a shift in the K-shell edge. Figure 4.4 illustrates how the 1s threshold moves to higer energies as electrons are progressively removed from iron.

K-shell absorptions are observed astronomically. Figure 4.5 reproduces the X-ray spectrum of the Crab Nebula, a supernova remnant. The X-ray spectrum has an intrinsic shape $I(E) = AE^{-2.08}$ [ph cm^{-2} s^{-1} keV^{-1}] with, superimposed on it, K-shell absorption by the various atoms in the gas. The depression near 0.5 keV can be plausibly attributed to the oxygen K-shell absorption.

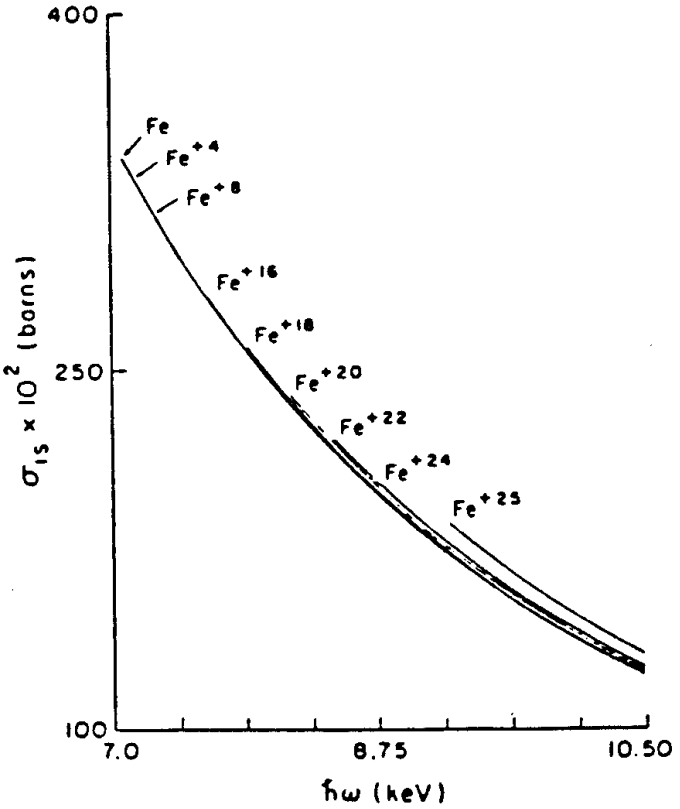

Figure 4.4– K-shell photoeffect cross sections for various Fe ions.

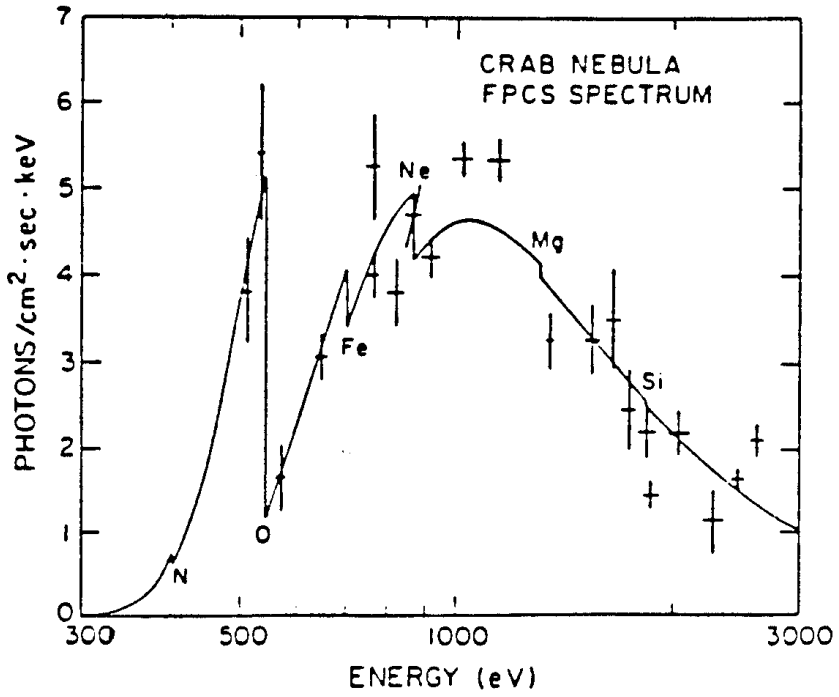

Figure 4.5– The X-ray spectrum of the Crab Nebula. The solid curve is a model fit, with the K-edges of N, O, Ne, Mg, and Si indicated along with the L-edge of Fe.

B. Recombination

1. Hydrogen

The process of photoionization has an inverse process called "radiative recombination"

$$H^+ + e(\epsilon) \rightarrow H(nl) + h\nu \tag{4.16}$$

where ϵ is the kinetic energy of the electron. A relation between the rates of the two processes can be derived in the same way as the relations between bound-bound absorption and emission probabilities by using the principle of detailed balance. If $\sigma_{ni}(\nu)$ is the cross section for photoionization of an atom initially in state n by a photon of frequency ν, then there is a corresponding cross section $\sigma_{nr}(\nu)$ for the capture of a free electron of kinetic energy $\epsilon = 1/2mv^2$ by the next ion in the appropriate state into state n of the atom. In order to conserve energy and angular momentum in the process, it is necessary that this capture be accompanied by creation of a photon of energy $h\nu' = 1/2mv^2 + |I_n|$, where I_n is the ionization energy of state n. Figure 4.6 illustrates the energetics of the process.

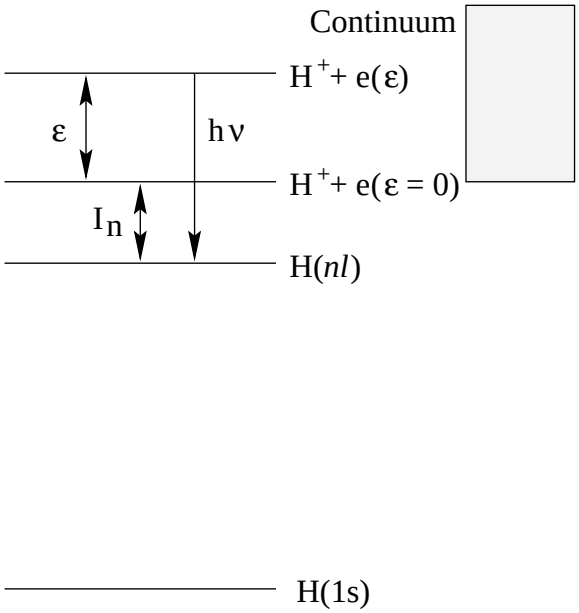

Figure 4.6– The energetics of radiative recombination to level nl of hydrogen under emission of a photon with frequency ν.

Clearly, $hd\nu' = mvdv$, and in thermodynamic equilibrium at temperature T we can insist that the rate of photoionization (including stimulated recombination)

$$\frac{4\pi B_\nu(T)}{h\nu}[1 - e^{-\mathrm{h}\nu/\mathrm{kT}}]\sigma_{ni}(\nu)d\nu \tag{4.17}$$

be exactly balanced by the rate of (spontaneous) recombination

$$v\sigma_{nr}(v)f(v)dv \tag{4.18}$$

where

$$f(v)dv \;=\; 4\pi^{-1/2}\left(\frac{m}{2k\mathrm{T}}\right)^{3/2/} v^2 e^{-\mathrm{mv}^2/2\mathrm{kT}}dv \tag{4.19}$$

is the Maxwell-Boltzmann distribution function,

$$B_\nu(\mathrm{T}) \;=\; \frac{2h\nu^3}{c^2}\cdot\frac{1}{e^{h\nu/k\mathrm{T}-1}} \tag{4.20}$$

is the Planck function, and

$$\frac{N(X^{i+1})N_e}{N(X^i)} \;=\; \frac{2g_{i+1}}{g_{i,n}}\left(\frac{2\pi m_e k\mathrm{T}}{h^2}\right)^{3/2} e^{-h\nu_0/k\mathrm{T}} \tag{4.21}$$

is the "Saha equation" relating the densities of the recombining and recombined ions, $N(X^{i+1})$ and $N(X^i)$ to the electron density in terms of the statistical weights g of the states considered and $h\nu_0 = |I_n|$. Thus, in thermodynamic equilibrium:

$$N_e N(X^{i+1}) v\sigma_{nr}(v) f(v) dv \;=\; (1-e^{-h\nu/k\mathrm{T}})N(X^i)\frac{4\pi B_\nu(\mathrm{T})}{h\nu}\sigma_{ni}dv \quad , \tag{4.22}$$

which simplifies to:

$$\sigma_{nr}(v) \;=\; \frac{g_{i,n}}{g_{i+1}}\cdot\left(\frac{h\nu}{mcv}\right)^2\cdot\sigma_{ni}(\nu) \tag{4.23}$$

a general relation independent of T. It is useful to define a recombination rate coefficient:

$$\alpha_n(\mathrm{T}) \;=\; \int_0^\infty \sigma_{nr}(v) v f(v) dv \qquad [\mathrm{cm^3 s^{-1}}] \tag{4.24}$$

that provides the total rate $N_e\alpha_n(\mathrm{T})$ $[\mathrm{s^{-1}}]$ at which electrons with a velocity distribution $vf(v)dv$ are captured. For purposes of describing the relative concentrations of different stages of ionization it is also useful to have a total recombination rate coefficient:

$$\alpha(\mathrm{T}) \;=\; \sum_n \alpha_n(\mathrm{T}). \qquad [\mathrm{cm^3 s^{-1}}] \tag{4.25}$$

In practice, for most atoms it is quite good enough to compute α_n for the lowest n directly from the photoionization cross sections and to use approximate hydrogenic values for higher n. See R. J. Gould (1978, *Ap. J.* **219**, 250).

Some useful results for $\mathrm{H^+} + e \rightarrow \mathrm{H(n)} + h\nu$ follow. The cross sections for hydrogen can, of course, be computed exactly using (4.23). Fitting formulae, which are accurate to within 1% for 2K < T < 64,000K:

$$\alpha(\mathrm{T}) \;=\; \sum_n \alpha_n(\mathrm{T}) \;=\; 10^{-11}\mathrm{T}^{-1/2}\left\{13.1119 - 2.15637x - 0.096628x^2 + 0.0181042x^3\right\} \tag{4.26}$$

and

$$\alpha_B(\mathrm{T}) = \sum_{n=2}^{\infty}\alpha_n(\mathrm{T}) \;=\; \alpha(\mathrm{T}) - \alpha_1(\mathrm{T}) \;=\; 10^{-13+y} \qquad [\mathrm{cm^3 s^{-1}}] \tag{4.27}$$

with x=$\log_{10}$T and

$$y = 3.07091 - 0.618352x + 0.0161247x^2 - 0.00710107x^3 \quad . \tag{4.28}$$

For temperatures around 10^4K, α can also be written:

$$\alpha_H \;\approx\; 4 \times 10^{-13} \left(\frac{10^4}{\mathrm{T}}\right)^{0.73} \qquad [\mathrm{cm^3 s^{-1}}] \quad . \tag{4.29}$$

The exact values are given in Table 4.9.

Table 4.9– Radiative recombination coefficients of H.

T_e(K)	500	1000	2500	5000	10,000	20,000	50,000
α(T)	3.11(-12)	1.99(-12)	1.08(-12)	6.73(-13)	4.12(-13)	2.48(-13)	1.22(-13)
α_B(T)	2.40(-12)	1.48(-12)	7.63(-13)	4.50(-13)	2.58(-13)	1.42(-13)	6.12(-14)

Note that the recombination process produces continuum emission and that the photon energy $h\nu$ is related to the velocity of the recombining electron v by $h\nu = mv^2/2 + |I_n|$. For a distribution of electron velocities $f(v)dv$, the resulting emissivity of hydrogen due to recombination is:

$$f_\nu \;\;=\;\; \frac{N(H^+)N(e)}{4\pi} \sum_{n=0}^{\infty} \sum_{l=0}^{n-1} v\sigma_{nl}(v) f(v) h\nu \frac{dv}{d\nu} \tag{4.30}$$

These photons have sufficient energy to ionize the product atom. However, with the exception of metastable H(2s) atoms in very dense nebulae, the equilibrium populations of the excited atoms is so low that the effect on the hydrogen ionization rate is negligible.

The recombination cross sections for hydrogen-like ions may be obtained from those for hydrogen by a simple scaling:

$$\alpha_Z(nl|\mathrm{T}) \;\;=\;\; Z\alpha_H(nl|t) \quad , \tag{4.31}$$

where t =T/Z^2.

2. Helium

a) radiative recombination

Just as for hydrogen, the He^+ ions produced by photoionization can undergo radiative recombination:

$$He^+ + e \rightarrow He^* + h\nu, \tag{4.32}$$

where He^* is any of the singlet or triplet states of helium. Because most of the recombinations take place into excited states, the recombination rate coefficients for helium are similar in magnitude to those for hydrogen. Values of the rate coefficients for recombination α_{He}(T), and of the rate coefficient $\alpha_{He}(1\ ^1\mathrm{S},\ \mathrm{T})$ for capture directly into the ground 1 $^1S_0$ state are given in Table 4.10. They can be represented by:

$$\alpha_{He}(\mathrm{T}) = 4.3 \times 10^{-13} \left(\frac{10^4}{\mathrm{T}}\right)^{0.672} \qquad [\mathrm{cm^3 s^{-1}}] \tag{4.33}$$

$$\alpha_{He}(1^1S, \mathrm{T}) = 1.6 \times 10^{-13} \left(\frac{10^4}{\mathrm{T}}\right)^{0.480} \qquad [\mathrm{cm^3 s^{-1}}] \tag{4.34}$$

Note that if helium is embedded in a gas composed mostly of hydrogen, the helium recombination radiation may be absorbed by hydrogen. In particular, all recombination of helium ions into excited singlet states, with the exception of the 2 ^{1}S state, are accompanied by the emission of photons that ionize hydrogen. Recombinations into the 2 ^{1}S state are followed by two-photon decay.

Table 4.10– He Radiative Recombination Coefficients [$\mathrm{cm^3 s^{-1}}$]

T_e(K)	5000	10,000	20,000
α_{He}	6.49(-13)	4.32(-13)	2.69(-13)
$\alpha_{He}(1\ ^1\mathrm{S})$	2.23(-13)	1.59(-13)	1.14(-13)

As Figure 3.2 shows, this spectrum peaks around 800 Å. On average, a fraction 0.56 of the decay photons has enough energy to ionize hydrogen. Three fourths of the captures result in triplet states, which decay rapidly into the long-lived 2 ^{3}S state. At low densities, the 2 ^{3}S states decays radiatively and the photons ionize hydrogen. At higher densities, the 2 ^{3}S state can be collisionally quenched so that no photons are produced.

b) dielectronic recombination

We have seen in IV A. 2. that helium (and also the heavier elements) has doubly-excited states embedded in the continuum due to the He^+ ion and free electron states, which give rise to auto ionization. Even more important astrophysically is the inverse process, inverse autoionization, or as it is more commonly known, "dielectronic recombination":

$$\mathrm{He}^+ + e \rightleftharpoons \mathrm{He}(nl, n'l') \rightarrow \mathrm{He}(n''l'', n'l') + h\nu. \tag{4.35}$$

Consider for example the 2s2p $^1\mathrm{P}^o$ state in He:

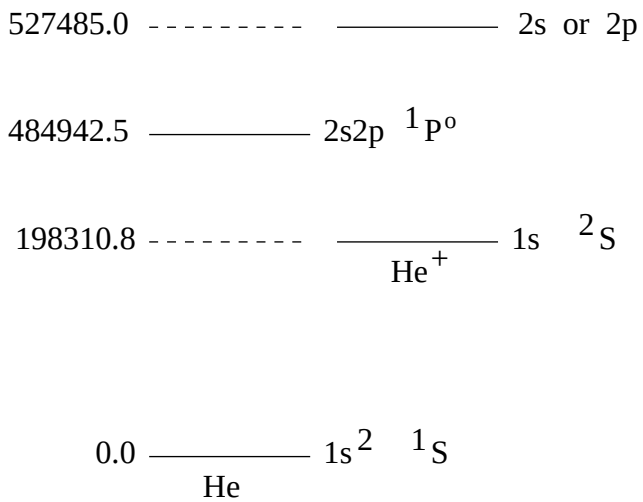

A free electron in the vicinity of a n=2 level of the He^+ ion can become "confused" about whether it is a free electron or whether it is one of the bound electrons in a doubly-excited He atom. There is, accordingly, a non-negligible probability for electron capture by an excited ion directly into a doubly-excited state of the corresponding next-lower

stage of ionization. The doubly-excited system can then either autoionize, or can undergo a radiative transition to a bound state, which is usually singly-excited. Thus, such a transition involves the transfer of the active electron from the nl orbital to the 1s orbital. These lines thus lie closer in wavelength to the nl-1s transitions of He^+, and are called "satellite lines". For example, the He 2s2p $^1P^o$ - 1s2s ^1S transition lies at 313.8 Å, whereas the He^+ 2p-1s transition occurs at 303.8 Å. Such satellite lines can be valuable diagnostics of high-temperature plasmas. Dielectronic recombination is important for He and for various Li-like ions in the solar corona, and has recently been shown to be significant in various abundant species in gaseous nebulae.

Dielectronic recombination can greatly enhance the total recombination rate. However, for helium all resonance states lie high in energy (the 2s2p ^3P state at 53.4 eV coincides in energy with an electron of kinetic energy 28.8 eV and a $He^+(1\ ^2S)$ ion). Thus dielectronic recombination of helium is significant only at high temperatures of the solar corona.

3. Other species

a) radiative recombination

Just like He, the ions of the other elements produced by photoionization can recombine by radiative recombination and by dielectronic recombination. The rate coefficients for radiative recombination are similar in magnitude to the values for hydrogenic systems with the same excess charge. This is because radiative recombination occurs into highly excited states which are hydrogen like. Of course, contributions from captures into occupied orbitals have to be excluded in the comparison with the hydrogenic systems. For temperatures near T=10^4K appropriate for nebulae, the rate coefficients may be represented by:

$$\alpha_A^R(\mathrm{T}) \quad = \quad C(10^4/\mathrm{T})^\eta \times 10^{-13} \qquad [\mathrm{cm^3 s^{-1}}] \ . \tag{4.36}$$

Values for C and η are given in Table 4.11 for several ions.

.

b) dielectronic recombination

Dielectronic recombination of heavier species occurs by the same steps as for the case of helium:
(i) A free electron collides with ion X^{m+} but remains captured in an outer excited state nl and forms with the excited core a doubly-excited state of $X^{(m-1)+}$. If autoionization occurs, the system returns to its original ionization state:

$$X^m + e \rightleftharpoons X^m(nl \ \rightarrow \ n'l') + e \tag{4.37}$$

(ii) the auto-ionizing state can be stabilized by a radiative transition either of the inner excited electron (at high temperatures) or by a radiative transition of the captured electron to a state below the first ionization limit of X^{m-1}:

$$X^{m-1}(nl,\ n'l') \rightarrow X^{m-1}(n_0 l_0,\ n'l') + h\nu \ \ . \tag{4.38}$$

Table 4.11– Rate Coefficients for Radiative Recombination
$(\alpha_A^R(\mathrm{T}) = C(10^4/\mathrm{T})^\eta \times 10^{-13} \quad [\mathrm{cm^3 s^{-1}}])$

Recombined System	A	C	η	A	C	η	A	C	η
C	4.7	0.624	C^+	23	0.645	C^{2+}	49	0.803	
N	3.9	0.608	N^+	22	0.639	N^{2+}	50	0.676	
O	3:3	0.678	O^+	20	0.646	O^{2+}	51	0.666	
Ne	2.8	0.759	Ne^+	15	0.693	Ne^{2+}	44	0.674	
Mg	2.6	0.855	Mg^+	8.8	0.838	Mg^{2+}	35	0.734	
Si	6.5	0.601	Si^+	10	0.786	Si^{2+}	37	0.693	
S	4.7	0.630	S^+	18	0.686	S^{2+}	22	0.745	
Fe	1.4	0.891	Fe^+	10	0.843	Fe^{2+}	33	0.746	
C^{3+}	92	0.791	C^{4+}	17	0.721				
N^{3+}	94	0.765	N^{4+}	157	0.780	N^{5+}	290	0.750	
O^{3+}	96	0.670	O^{4+}	159	0.759	O^{5+}	244	0.774	
Ne^{3+}	98	0.668	Ne^{4+}	150	0.684	Ne^{5+}	230	0.704	
Mg^{3+}	84	0.718	Mg^{4+}	140	0.716	Mg^{5+}	230	0.695	
Si^{3+}	73	0.735	Si^{4+}	120	0.735	Si^{5+}	210	0.716	
S^{3+}	70	0.755	S^{4+}	120	0.701	S^{5+}	170	0.849	
Fe^{3+}	78	0.682	Fe^{4+}	151	0.699	Fe^{5+}	262	0.728	

This process produces the dielectronic satellite lines of the parent ion line $nl \rightarrow n_0 l_0$. If the transition is to a state above the first ionization limit, a "secondary autoionization" can occur.

(iii) after the inital stabilizing transition has occurred, the singly excited state cascades down to the ground state:

$$X^{m-1}(n_0 l_0,\ n'l') \rightarrow X^{m-1}(n_0 l_0,\ n_0' l_0') + h\nu' + h\nu'' + ... \tag{4.39}$$

Thus, a characteristic line spectrum will occur.

The calculations of the rate coefficients for dielectronic recombinations are far from simple. They involve many specific computations of the energy level structure of both singly and doubly excited states, and of the probabilities of autoionization and radiative decay. At high temperatures, where recombination occurs mostly into core-excited resonance states, a general formula exists which is quite successful. At low temperatures, detailed and demanding computations appear necessary. Accurate results have been obtained for a number of ions. For T between 5000 and 15,000K, they can be reproduced approximately by:

$$\alpha_A^D(\mathrm{T}) \quad = \quad C(10^4/\mathrm{T})^\eta e^{-10^4 f/\mathrm{T}} \tag{4.40}$$

Values for these coefficients are given in Table 4.12.

The total recombination coefficient of species A may be approximated by

$$\alpha_A^{tot}(\mathrm{T}) \quad = \quad \alpha_A^R(\mathrm{T}) + \alpha_A^D(\mathrm{T}) + \alpha_A B(\mathrm{T}) \quad , \tag{4.41}$$

where $\alpha_A^B(\mathrm{T})$ is the contribution from the core-excited resonance captures. For ions of low excess charge, $\alpha_A^R(\mathrm{T})$ is largest at low temperatures, and $\alpha_A^B(\mathrm{T})$ dominates at high temperatures. However, at intermediate temperatures appropriate to nebulae, $\alpha_A^D(\mathrm{T})$ is often the largest term, as Table 4.13 illustrates.

c) example

Consider the dielectronic recombination of O^{4+}, with ground state configuration $1s^2 2s^2$. The doubly excited O^{3+} $^2F^o$ $1s^2 2p^2 3p$ state lies 486 cm^{-1} above the O^{3+} ionization limit. Thus, the O^{4+} ion can capture an electron with an energy near 0.6 eV into the $^2F^o$ state of O^{3+}, which then radiates to the stable O^{3+} ^2D $1s^2 2s 2p^2$ state in a transition in which the outer electron is transferred from the 3p orbital to the 2s orbital.

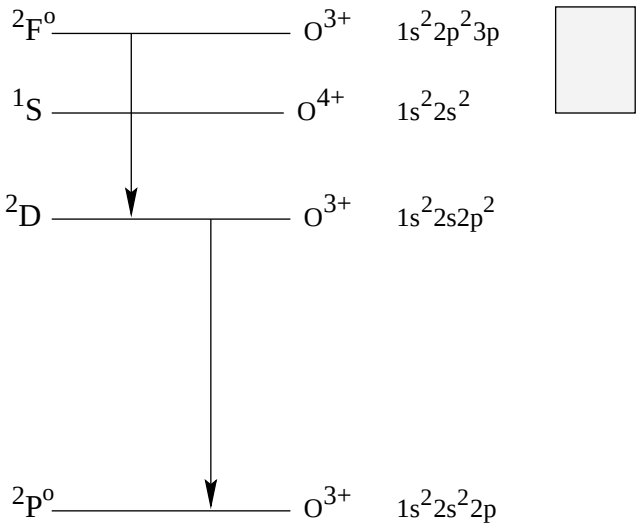

References for recombination rates:

Aldrovandi & Pequinot 1973, *Astron, Astrophys.* **25**, 137
Pequinot & Aldrovandi 1986, *Astron. Astrophys.* **161**, 169*
Tarter 1971, *Ap. J.* **168**, 313; 1973 *Ap. J.* **181**, 607
Weisheit 1973, *Ap. J.* **185**, 877

* beware of possible errors in their discussion of ionization rates.

Table 4.12– C and η Values for Dielectronic Recombination Coefficients [α_A^D(T) in eq. (4.40), 10^{-13} cm^{3}s^{-1}]

Recombined System A	C	η	f	A	C	η	f
C	1.58	-0.034	-0.1127	O^{2+}	378	1.128	1.1899
C^+	114	1.256	0.5960	Ne^+	6.91	0.337	0.4516
C^{2+}	202	1.339	0.4101	Ne^{2+}	352	1.200	0.2313
N	8.15	1.317	0.4398	Ne^{3+}	220	0.807	0.1702
N^+	36.5	0.306	0.5946	Ne^{4+}	762	0.998	0.1942
N^{2+}	401	0.779	0.6127	Mg	35.7	0.098	0.6260
O	1.16	0.344	0.4106	Al	19.1	0.330	0.2276
O^+	22.1	0.903	0.2769	Si	4.80	1.325	0.1342

Table 4.13– Radiative and Dielectronic Recombination Coefficients at T = 10^4 K [10^{-12} cm^{3}s^{-1}]

Recombined species A	α_A^R	α_A^D	Sum
C	0.47	0.18	0.64
C^+	2.3	6.1	8.4
C^{2+}	4.9	13	18
N	0.39	0.52	0.91
N^+	2.2	2.0	4.2
N^{2+}	5.0	2.2	27
O	0.33	0.08	0.41
O^+	2.0	1.7	3.7
O^{2+}	5.1	11	16
Ne	0.28	--	0.28
Ne^+	1.5	0.45	1.9
Ne^{2+}	4.4	27	31

IV Photoionization and Recombination (continued)

C. Accidental Resonance Fluorescence

It sometimes occurs that the frequencies of allowed transitions in different atoms or molecules are nearly equal. If one of the transitions belongs to an abundant atom and has a high intensity in some astrophysical environment, then the other species can "see" an anomalously intense radiation field at its transition and thus suffer an unusually high rate of radiative excitation. A few important examples are described below.

a) Bowen fluorescence for O III

There is an accidental coincidence between the wavelength of the He II Ly α line (1s-2p) at λ=303.78 Å and the O III $2p^2\ {}^3P_2$ line at λ=303.80 Å. This wavelength difference corresponds to the Doppler shift for a velocity of about 20 km s^{-1}. In most photoionized nebulae, the line widths are typically this large or larger, so that this degree of coincidence is for practical purposes exact.

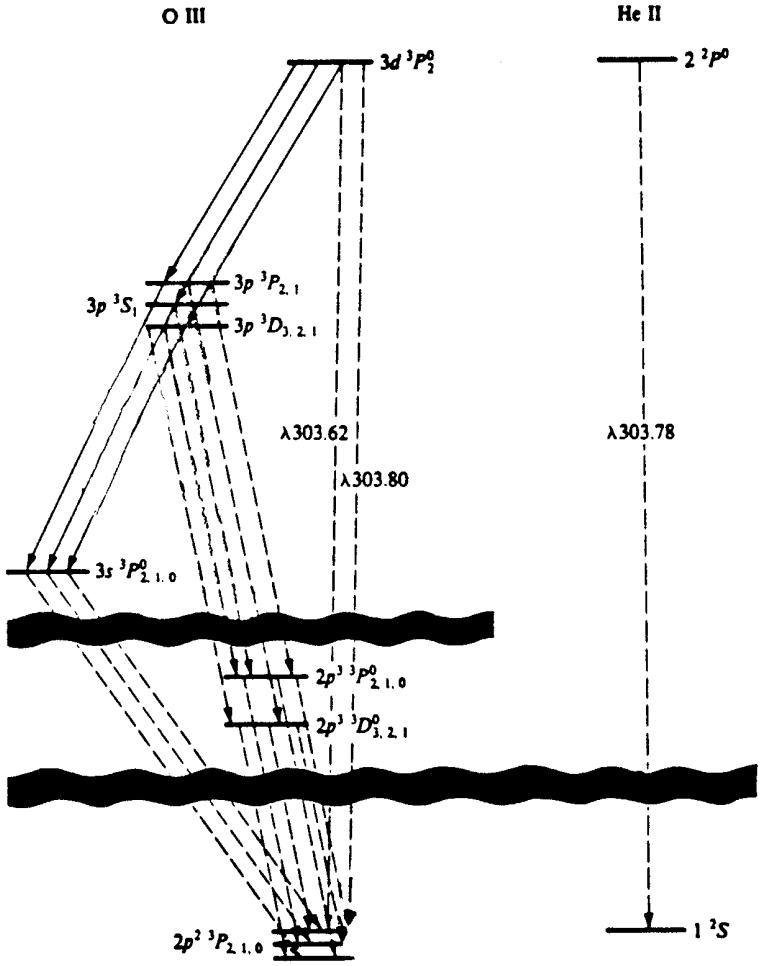

Figure 4.7– Schematic partial energy level diagrams of O III and He II showing the coincidence of the He II Ly α and O III $2p^2\ {}^3P_2$ – $2p3d\ {}^3P^o_2$ transitions near 303.80 Å. The Bowen resonance-fluorescence lines in the optical and near-UV are shown by the solid lines, while the far-UV transitions that lead to excitatio are indicated by dashed lines.

Table 4.14– O III Resonance-Fluorescence Lines

Transition	Wavelength (Å)	Relative probability	Relative intensity
$3p\ ^3P_2 - 3d\ ^3P_2^0$	3444.10	3.74×10^{-3}	0.277
$3p\ ^3P_1 - 3d\ ^3P_2^0$	3428.67	1.25×10^{-3}	0.093
$3p\ ^3S_1 - 3d\ ^3P_2^0$	3132.86	1.23×10^{-2}	1.000
$3p\ ^3D_3 - 3d\ ^3P_2^0$	2837.17	1.16×10^{-3}	0.104
$3p\ ^3D_2 - 3d\ ^3P_2^0$	2819.57	2.08×10^{-4}	0.019
$3p\ ^3D_1 - 3d\ ^3P_2^0$	2808.77	1.38×10^{-5}	0.0013
$3s\ ^3P_2^0 - 3p\ ^3S_1$	3340.74	1.79×10^{-3}	0.136
$3s\ ^3P_1^0 - 3p\ ^3S_1$	3312.30	1.07×10^{-3}	0.082
$3s\ ^3P_0^0 - 3p\ ^3S_1$	3299.36	3.57×10^{-4}	0.028
$3s\ ^3P_2^0 - 3p\ ^3P_2$	3047.13	2.14×10^{-3}	0.179
$3s\ ^3P_1^0 - 3p\ ^3P_2$	3023.45	7.12×10^{-4}	0.060
$3s\ ^3P_2^0 - 3p\ ^3P_1$	3059.30	3.95×10^{-4}	0.033
$3s\ ^3P_1^0 - 3p\ ^3P_1$	3035.43	2.37×10^{-4}	0.020
$3s\ ^3P_0^0 - 3p\ ^3P_1$	3024.57	3.17×10^{-4}	0.027
$3s\ ^3P_0^0 - 3p\ ^3D_1$	3757.21	3.57×10^{-6}	0.0002
$3s\ ^3P_1^0 - 3p\ ^3D_1$	3774.00	2.67×10^{-6}	0.0002
$3s\ ^3P_2^0 - 3p\ ^3D_1$	3810.96	1.80×10^{-7}	0.0001
$3s\ ^3P_1^0 - 3p\ ^3D_2$	3754.67	7.22×10^{-5}	0.0049
$3s\ ^3P_2^0 - 3p\ ^3D_2$	3791.26	2.41×10^{-5}	0.0016
$3s\ ^3P_2^0 - 3p\ ^3D_3$	3759.87	5.39×10^{-4}	0.037

He is the second most abundant element, and in high-excitation nebulae, He^+ or He^{++} can be the dominant stage of ionization. In those same regions, O^{++} will be abundant. Both the He II and the O III λ=303.8 Å lines are "resonance transitions" meaning the ground states, which are the most populous, are the lower states of the transitions.

The He^+ ions can also re-absorb their own line photons many times before they escape from the nebulae. The absorptions by O^{++} ions can be a significant contribution to the removal of the He^+ Ly α photons.

What happens to the O^{2+} following excitation to the 3d $^3P_2^o$ level? The most likely process is simply radiative decay back to the $2p^2\ ^3P_2$ level in the same λ 303.80 Å line. This occurs about 74% of the time. The next most likely decay process, with a probability of 24%, is emission of the $2p^2\ ^3P_1$ - 3d $^3P_2^o$ line at λ 303.62 Å. Finally, in 2% of the cases, the 3d $^3P_2^o$ level will decay by emitting one of the six longer wavelength photons in the 3p ^{3}Ly - 3d $^3P_2^o$ transitions illustrated in Figure 4.7. The various terms in the 3p configuration subsequently decay through various 3s $^3P^o$ - 3p ^{3}Ly lines lying between 3400 and 3800 Å. Thus, a characteristic spectrum results, and the cascade lines in the near-ultraviolet and visible wavelength range are prominent features of planetary nebulae and other high excitation sources, such as optical counterparts of X-ray sources.

The proper interpretation of the line requires a careful treatment of the problem of the scattering, escape and destruction of the He II Ly α photons. For example, a competing

process that destroys He II Ly α photons before they can be converted to O III Bowen resonance-fluorescence photons is absorption due to photoionization of H and He. Detailed calculations suggest that about 50% of the He II Ly α photons are eventually converted into Bowen resonance-fluorescence photons. These photons are distributed among the various individual lines as indicated in Table 4.14, in which the relative intensities are normalized to λ 3133 Å.

References:
Osterbrock, D. 1987, pp. 107-111.
Flower and Perinotto 1980, *MNRAS* **191**, 301-8
Kallman and McCray 1980, *Ap. J.* **242**, 615
Sternberg and Dalgarno 1987, *Comm. on Astrophys.*

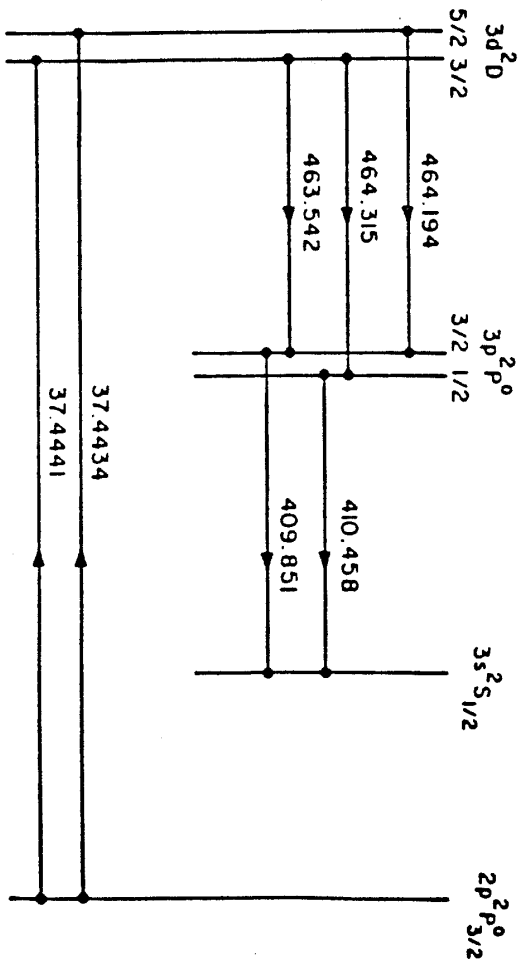

Figure 4.8– The fluorescence spectrum of N^{2+} produced by absorption in the transition 2p $^2P^o_{3/2}$ - 3d ^2D (λ in nm).

A further remarkable coincidence occurs following the excitation of O^{++}: one of the lines emitted in the cascade from the 3d $^3P^o_2$ level, the $2p^2$ $^3P_2$ - 2p3s $^3P_1{}^o$ line at 374.436 Å, can be absorbed by the 2p $^2P^o_{3/2}$ - 3d ^2D transition of N^{++}, giving rise to emission lines between 4635 and 4643 Å. These cascade lines are illustrated in Figure 4.8.

b) H Ly β and O I

The lines of H Ly β (1s - 3p) λ=1025.722 and O I $^3P_2$ - 3d $^3D^o_3$, λ=1025.7618 Å agree within 11.6 km/s in Doppler velocity shift at that wavelength. The excitation of O I by H Ly β leads with fairly high probability to the emission of the O I 3d $^3D^o$ - 3p ^3P lines at λ=11287 Å, and the 3p ^3P - 3s $^3S^o_1$ lines at 8446 Å.

Such fluorescent emission is seen in nebulae, comets, active galaxies, novae and the solar chromosphere. As we will see later, Ly β can also drive some interesting molecular fluorescence processes.

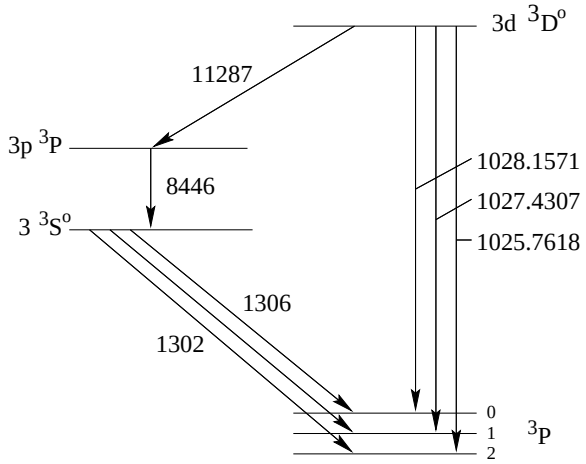

Figure 4.9– The fluorescence spectrum of O produced by absorption in the ^3P - 3d $^3D^o$ transition (λ in Å).

References:

Grandi 1980, *Ap. J.* **328**, 10

Thompson *etal.*, 1978, *Ap. J. Letters* **222**, L49

Skelton and Shine 1982, *Ap. J.* **259**, 269

Strittmatter *etal.* 1977, *Ap. J.* **216**, 23.

c) H Ly β and Mg II

The H Ly β (1s-3p) line at 1025.722 Å also nearly coincides with the Mg II 3 $^2S_{1/2}$ - 5 $^2P_{3/2}$, $^2P_{1/2}$ lines at λ=1025.9681 and 1026.1133 Å, respectively. The shifts of these lines are 71.85 and 114.29 km/s, respectively, so that the absorption occurs mostly in the long wavelength wing of the Ly β profile. This pumping mechanism can excite a number of Mg II f luorescence lines, most prominently at 3848, 3850; 7877, 7896; 8214, 8235; 9218, 9244 Å; and 2.1, 2.4 μm.

Because these are all doublet levels, line intensities within multiplets will be sensitive to the relative rates of absorption in the two 3s-5p resonance lines, and thus to the shape of the Ly β line profile:

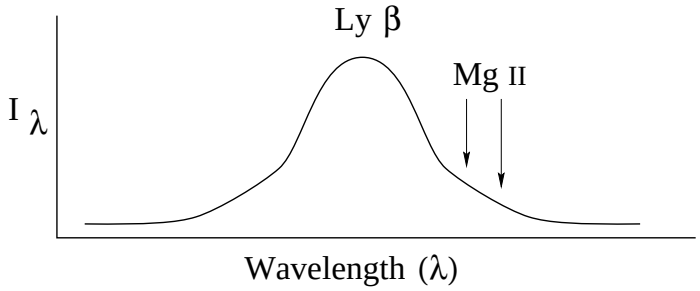

D. Absorption and emission of line radiation

Consider first the simple, idealized case of a source of continuum radiation viewed through a uniform plane-parallel slab of cool, absorbing gas. Some of the background light can be absorbed in passing through the intervening slab at frequencies at which the atoms have allowed transitions, non-negligible populations in the lower states, (and without a greater population in the upper state.) An absorbed photon, of course, can be re-emitted at the "same" transition frequency, but because this spontaneous emission is isotropic (independent of direction), the fraction of fluorescent photons emerging in the same direction (that is, toward the observer), as the absorbed photons is negligible. We want to describe in detail how the strength of the absorbtion is related to the abundance of the absorbing atom and to its atomic properties.

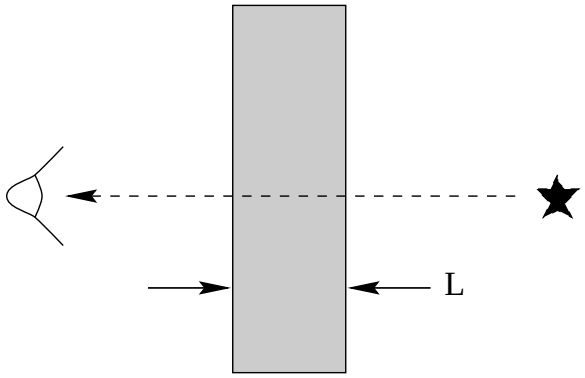

Let $I_\nu(0)$ = intensity of background light as a function of ν near a spectral line.
I_ν = observed intensity; including absorption.
s = linear distance through slab
ν_0 = central frequency of transition
In this simple case of pure absorption

$$\frac{dI_\nu}{ds} = -n_l \sigma_{lu}(\nu) I_\nu \tag{4.42}$$

where n_l is the concentration in cm^{-3} in the lower state of the transition $u \leftarrow l$ and $\sigma_{ul}(\nu)$ is the cross section for absorption in the transition. Because we are assuming a uniform absorbing medium, only $I_\nu(s)$ depends on the postion within the slab, and a simple change of variable is possible:

$$\frac{dI_\nu}{d\tau} = -I_\nu \tag{4.43}$$

where $d\tau_\nu = n_l \sigma_{lu}(\nu) ds$ is the dimensionless "optical depth". The solution to this simple differential equation is:

$$I_\nu \;=\; I_\nu(0) e^{-\tau_\nu} \quad . \tag{4.44}$$

For a uniform slab $\tau_\nu = (n_l L)\sigma(\nu)$ where $n_l L = N_l$ is the "column density" of absorbers in cm^{-2} through the whole slab of thickness L.

The frequency dependence of τ_ν for an isolated spectral line depends upon the line broadening mechanisms. We have already seen that a spectral line has a finite extent in frequency simply due to the finite lifetime of the upper state which corresponds to an uncertainty in its energy. This gives rise to a Lorentzian function (the Fourier transform of an exponential decay):

$$\phi_L(\nu - \nu_0) \;=\; \frac{(\alpha_L/\pi)}{\alpha_L^2 \;+\; (\nu - \nu_0)^2} \tag{4.45}$$

in terms of a "damping" width:

$$\alpha_L \;=\; \sum_{l'} A_{ul'}/4\pi \qquad [\mathrm{Hz}]. \tag{4.46}$$

In real gases, there will usually be another important contribution to the line broadening due to the motions of the absorbing atoms, which, due to the distribution of "Doppler Shifts"

$$\frac{\delta\nu}{\nu} \;=\; \frac{\delta v}{c} \tag{4.47}$$

allow the atoms to absorb over some finite distribution of frequencies. Microscopically, this is usually thermal Doppler broadening with a Maxwellian distribution of speeds characterized by a temperature T. In astrophysical contexts, there are often additional microscopic or macroscopic motions that enlarge the broadening. As long as these motions are basically random, the combined effect can still be well-characterized by a Maxwellian distribution at some effective Doppler temperature T_D. This gives rise to a Gaussian profile function:

$$\phi_D(\nu - \nu_0) \;=\; \frac{1}{\pi^{1/2}\alpha_D} e^{-ln2\left(\frac{\nu-\nu_0}{\alpha_D}\right)^2} \quad , \tag{4.48}$$

$$\alpha_D \;=\; \frac{\nu_0}{c}\left[\frac{2k\mathrm{T}_D}{M} ln2\right]^{1/2} \tag{4.49}$$

is the 'half-width" at half-maximum and M is the mass of the absorber. With M in amu:

$$\alpha \;=\; 3.5825 \times 10^{-7} \nu_0 (\mathrm{T}_D/M_{\mathrm{amu}})^{1/2} \qquad [\mathrm{Hz}] \tag{4.50}$$

In the astronomical literature, one often encounters the "full-width" at half peak (FWHM) intensity of the Gaussian function in velocity units:

$$\Delta v \;=\; \frac{2c}{\nu_0}\alpha_D \tag{4.51}$$

or a "Doppler parameter" in velocity units:

$$b \equiv \alpha_D \frac{c}{\nu_0} ln2^{-1/2} = \frac{\Delta v}{2(ln2)^{1/2}} = \frac{\Delta v}{1.665} \quad . \tag{4.52}$$

For a Gaussian function $\phi(v)$ with Δv = FWHM, the area under the curve is given by:

$$\int \phi(v) dv = \frac{\phi_{max} \Delta v}{0.93943728} = 1.064467 \phi_{max} \Delta v \quad . \tag{4.53}$$

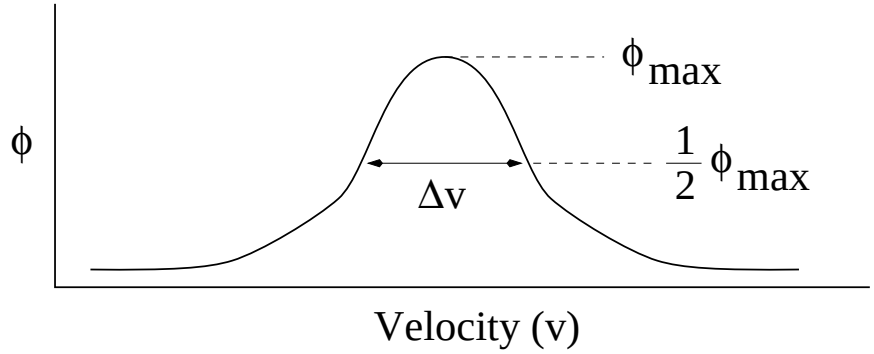

In general, the overall line profile (that is, the frequency dependence of the absorption cross section) will be the convolution of ϕ_L and ϕ_D. This convolution of Lorentzian and Gaussian functions is called a "Voigt function", which we will write in terms of the dimensionless relative line frequency:

$$x = \frac{\nu - \nu_0}{\alpha_D} (ln2)^{1/2} \tag{4.54}$$

and the linewidth ratio

$$y = \frac{\alpha_L}{\alpha_D} (ln2)^{1/2} \tag{4.55}$$

to be

$$k(x,y) = \frac{y}{\pi} \int_{-\infty}^{\infty} \frac{e^{-t^2}}{y^2 + (x-t)^2} dt \quad . \tag{4.56}$$

The Voigt function is defined as normalized such that:

$$\int_{-\infty}^{\infty} k(x,y) dx = \pi^{1/2} \tag{4.57}$$

and the optical depth can then be written:

$$\tau_\nu = n_l L \sigma_0 k(x,y) \quad , \tag{4.58}$$

where the line-center absorption cross-section σ_0 can be determined from the oscillator strength:

$$\int_{-\infty}^{\infty} \sigma(\nu) d\nu = \frac{\pi e^2}{m_e c} f_{lu} = \int_{-\infty}^{\infty} \sigma k(x,y) d\nu \tag{4.59}$$

Using $dx = (ln2)^{1/2}/\alpha_D dnu$, then:

$$\sigma_0 = \frac{\pi e^2}{m_e c}\left(\frac{ln2}{\pi}\right)^{1/2}\frac{f_{lu}}{\alpha_D} = 0.012466\frac{f_{lu}}{\alpha_D} \quad [\mathrm{cm}^2] \; . \tag{4.60}$$

In many real observations, there is insufficent resolution to see the full structure of the line profile, and one is forced to deal with an integrated line strength called the "equivalent width", W_{nu}.

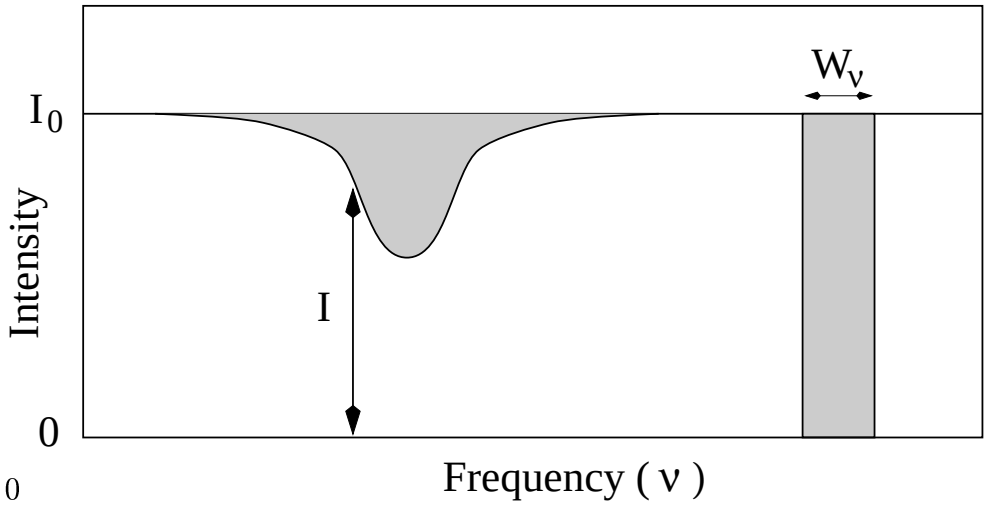

Figure 4.10– The equivalent width W_ν of a line.

$$W_\nu \equiv \int_{-\infty}^{\infty}(1-e^{-\tau_\nu})d\nu \quad [Hz] \tag{4.61}$$

$$\equiv \int_{-\infty}^{\infty}\left[\frac{I_\nu(0)-I_\nu}{I_\nu(0)}\right]d\nu \; .$$

W_ν can be thought of as the width of a rectangular profile extending from $I_\nu = 0$ to $I_\nu = I_\nu(0)$ that has the same area as the actual line (see Figure 4.10). The equivalent width is also often expressed in wavelength units:

$$W_\lambda = \left|\frac{d\lambda}{d\nu}\right| W_\nu = \frac{\lambda^2}{c}W_\nu \quad [\mathrm{cm}] \tag{4.62}$$

The measured equivalent width can be related to the column density of absorbers through the so-called "curve-of-growth", which is illustrated in Figure 4.11.

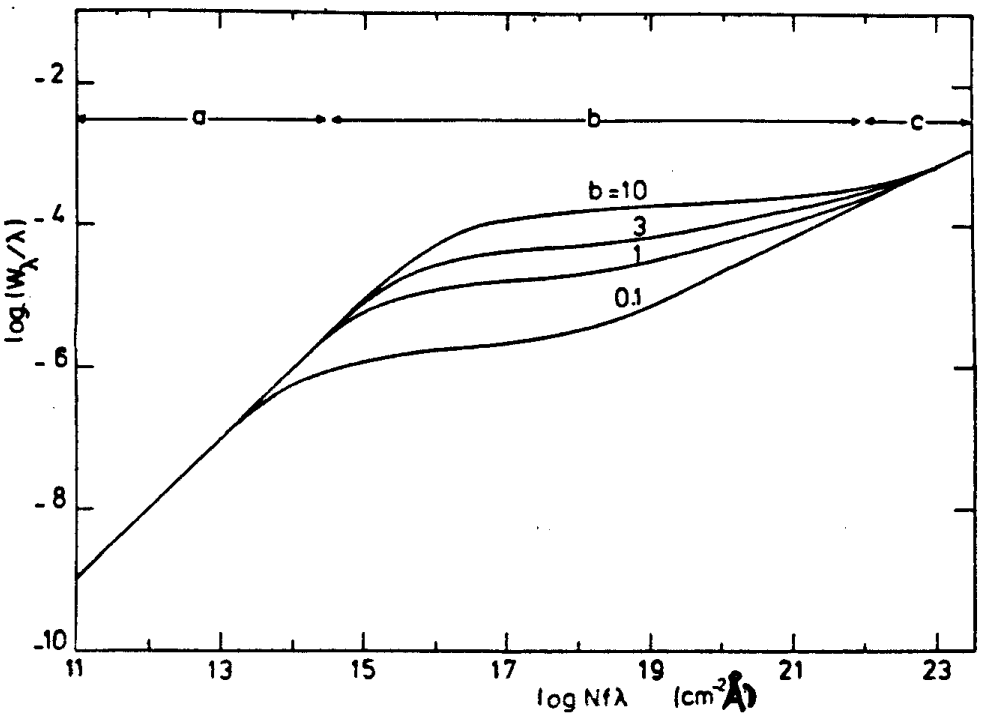

Figure 4.11– Illustration of a general curve of growth. a: linear part, b: flat part, c: square-root part.

This characteristic behavior falls into three regimes:

I. In the limit of extremely weak lines, $\tau_0 << 1$, and:

$$W_\nu \simeq \int_{-\infty}^{\infty} \tau_\nu d\nu \simeq N_l \int_{-\infty}^{\infty} \sigma(\nu) d\nu = \frac{\pi e^2}{m_e c} N_l f_{ul} \tag{4.63}$$

Thus, in this linear regime, W_ν is directly proportional to the column density in the lower level N_l. If W_λ and λ are in Å, the relation becomes

$$N_l = 1.13 \times 10^{20} \frac{W_\lambda}{f_{lu}\lambda^2} \qquad [\mathrm{cm}^{-2}] \tag{4.64}$$

II. With increasing absorption (large τ_0), the point is reached where virtually all background light has been absorbed near line center, but far away from line center the absorption cross section is orders of magnitude smaller, so that absorption in the line wings is a negligible contribution to the total absorption; in this regime the equivalent width increases only very slowly with increasing column density. Alternatively, this means that a column density derived from a measured equivalent width in this regime is likely to be rather uncertain unless the measurement errors are exceedingly small and the Doppler width is well established. The onset of this "flat part" of the curve of growth depends on both the Doppler width and the column density. For example, the deviation from the linear relation (4.63) exceeds 10% when

$$\frac{N_l f_{lu} \lambda}{b} > 1.87 \times 10^{14} \qquad [\mathrm{s}^{-1}] \tag{4.65}$$

for λ in Å, $b = \Delta v/1.665$ in km/s, and N_l in cm^{-2}.

III. In the form of the curve of growth of Figure 4.11, where $\log(\mathrm{W}_\lambda/\lambda)$ is plotted vs. $\log(\mathrm{Nf}\lambda)$, the curve is virtually independent of the properties of the particular absorber until the "damping" or "square-root" part is reached. Here the Lorentzian wings of the line profile dominate the additional absorption with increasing column density. Thus, the absorption depends on α_L, which contains the total lifetime of the upper level. The contributions due to the extreme wings can be determined from the asymptotic form

$$\tau_x \quad \sim \quad nL\sigma_0(y/\pi)^{1/2}\ x^{-2} \tag{4.66}$$

which leads to a square-root relation between column density and equivalent width.

There is an additional kind of broadening that results from the perturbations of energy levels and lifetimes by "collisions" with other particles in a dense gas. This is usually called "pressure broadening" or "collision broadening". There are at least 3 categories of theories used to describe this: 2 of these are approximate theories for limiting cases, called "quasi-static" and "impact" theories, and the other is an attempt at a completely quantum thoery of line broadening. Note that line broadening effects can often be measured directly.

One theory considers a collision which interrupts the emission of a radiating atom:

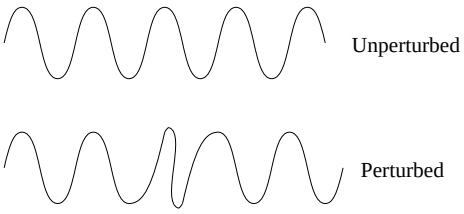

This produces a random phase shift, which manifests itself as a broadening of the frequency distribution of emitters when the random phase interruptions are averaged over an "ensemble" (a whole lot) of emitting atoms and collision partners. If these perturbing collisions are characterized by a collision frequency Γ_{coll}, then the Lorentzian part of the line broadening is given by a total width

$$\Gamma = \Gamma_{natural} + 2\Gamma_{coll} \tag{4.67}$$

where $\Gamma_{natural} = \Sigma \mathrm{A}_{ul} = 1/\tau_{rad}$ is the natural line width. Clearly, Γ_{coll} must depend on (a) the cross section for "phase interruption"; (b) gas density; (c) gas temperature (that is, the speed of the colliding particles).

Alternatively, one can think of the ions, atoms and electrons in a dense gas as creating an average external electric field around an atom. This quasi-static Stark effect then weakly perturbs the energy levels of the radiating atom and gives rise to Lorentzian line broadening. For this reason pressure broadening is sometimes called "Stark broadening".

The broadening due to the radiative lifetime of the upper state and collisions is also known as a homogeneous form of line broadening; each molecule may absorb or emit radiation over the entire linewidth. A homogenous line nearly always has a Lorentzian shape. It is really a reflection of the Heisenberg uncertainty principle; some decay process prevents the molecule from remaining in a specified energy state for longer that Δt, on the average, and the line width is $\Gamma = 1/\Delta t$.

The Doppler broadening of the line is known as inhomogeneous broadening. Figure 4.12 compares the Gaussian and Lorentzian line shapes. Note that if a species has a number of closely spaced lines, each of which has its own homogeneous line shape, the result of which has its own homogeneous line shape, as illustrated in Figure 4.13.

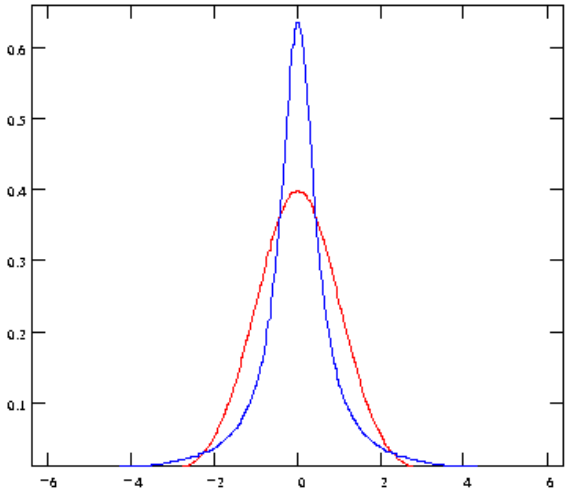

Figure 4.12– A comparison of normalized lorentzian and gaussian lines with the same integrated area, for which the gaussian shape has a higher maximum intensity, but where the lorentzian line shape has much more absorption (or emission) in the far line wings.

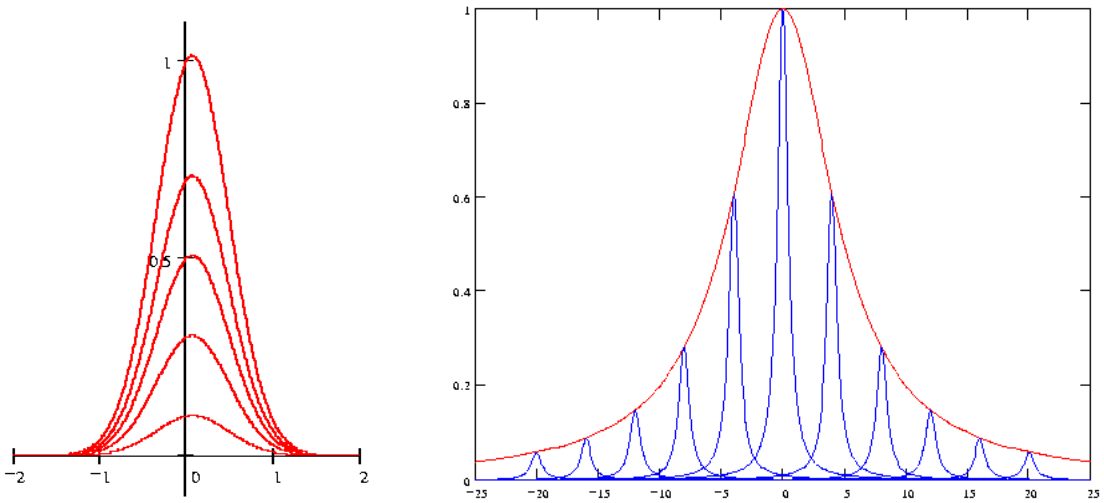

Figure 4.13– Homogeneous (left) versus inhomogeneous (right) lineshapes. For a homogeneous transition, excitation in any one part of the line profile results in an interaction with all of the atoms or molecules in the sample. For a inhomogeneous transition, the total line shape is composed of a number of sub-populations with their own intrinsic (homogeneous) line shape that are slightly displaced in frequency with respect to each other.